Heterogeneous catalysis

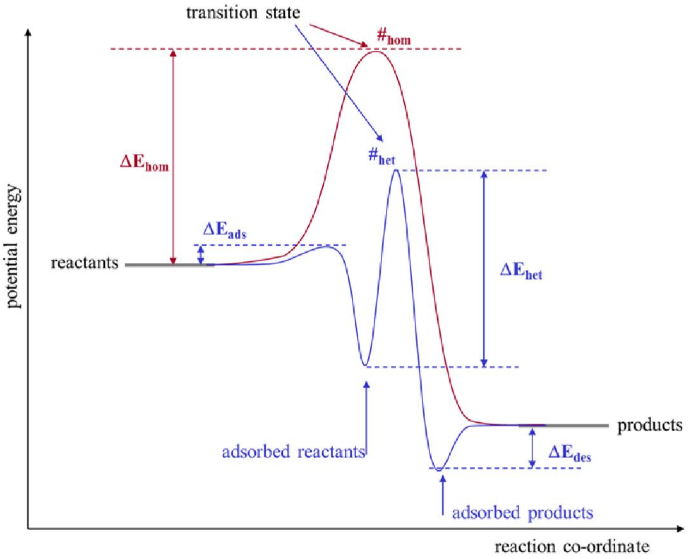

Heterogeneous catalyst

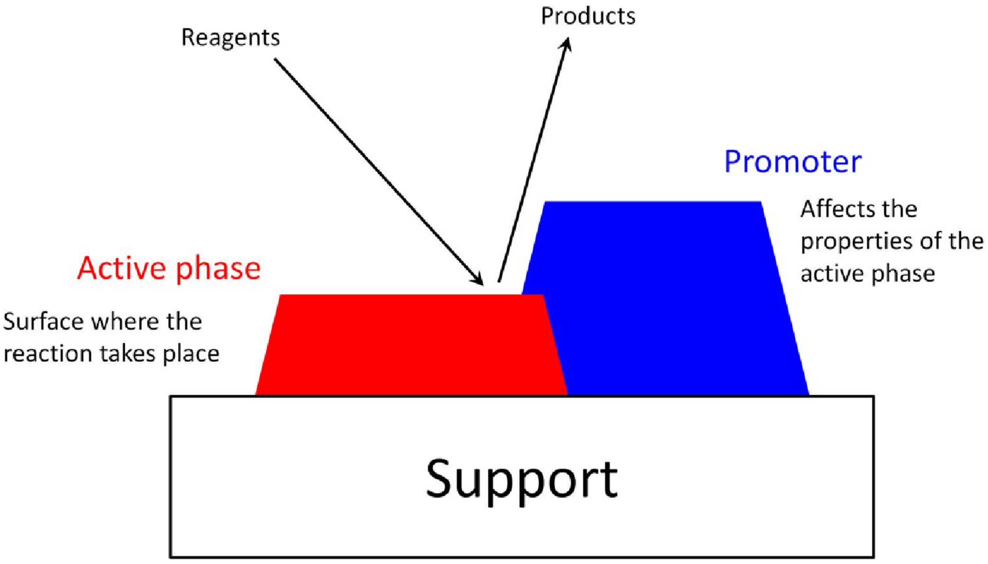

Reagents

Products

Promoter

Affects the
properties of the
active phase

Active phase

Surface where the
reaction takes place

Support

Bonding to surfaces

When atoms or molecules adsorb on ordered crystal surface, they usually form ordered surface structure over a wide range of temperature and surface coverages.

Two factors which decide the surface ordering of adsorbates are Adsorbate-adsorbate (AA) interaction and adsorbate-substrate (AS) interaction

Chemisorption – adsorbate-substrate interaction is stronger than adsorbate-adsorbate interaction, so the adsorbate locations are determined by the optimum adsorbate-substrate bonding, while adsorbate-adsorbate interaction decides the long-range ordering of the overlayer.

Physisorption or physical adsorption – AA interaction dominates the AS interaction – the surface could exhibit incommensurate structures.

Bonding to surfaces

Two classifications distinguished by the magnitude of their enthalpies of adsorption

- ➢Physisorption: long-range but weak van der Waals-type interactions with negligible exchange of electrons and enthalpies~ΔH_{cond} ($-\Delta H_{AD}<35$ kJ/mol)
- ➢Chemisorption: formation of a chemical bond (covalent, ionic, metallic) with exchange of electrons and $-\Delta H_{AD}>35$ kJ/mol

Enthalpy of chemisorption depends strongly on surface coverage (interactions)

Precursor state

If adsorbate collides with the surface and doesn’t stick, it may not simply rebound, but rather form a weak bond (physisorption) and diffuse for a period (losing energy) until a vacant site is located for chemisorption to occur.

For adsorption to proceed, the gas needs to “dump” energy into the solid, if not it will desorb. The longer the gas molecule resides on the surface, the more likely is energy exchange with the surface. Can write an Arrhenius-type relationship between residence time and the enthalpy of adsorption at the precursor adsorption site.

Lennard-Jones Potential for physisorption

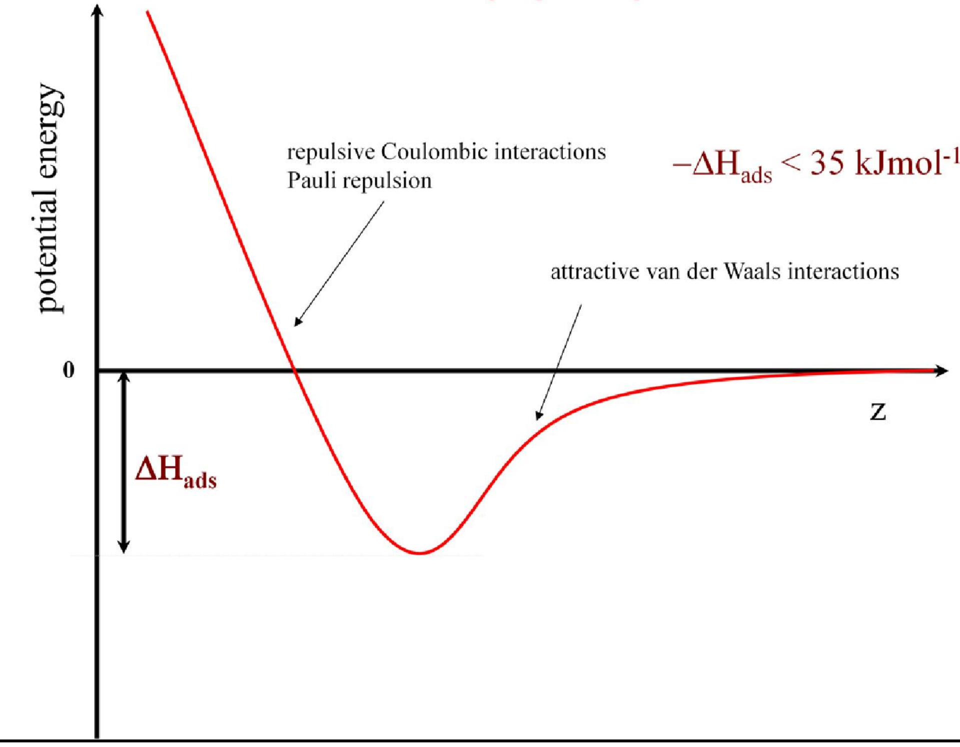

Potential energy profiles

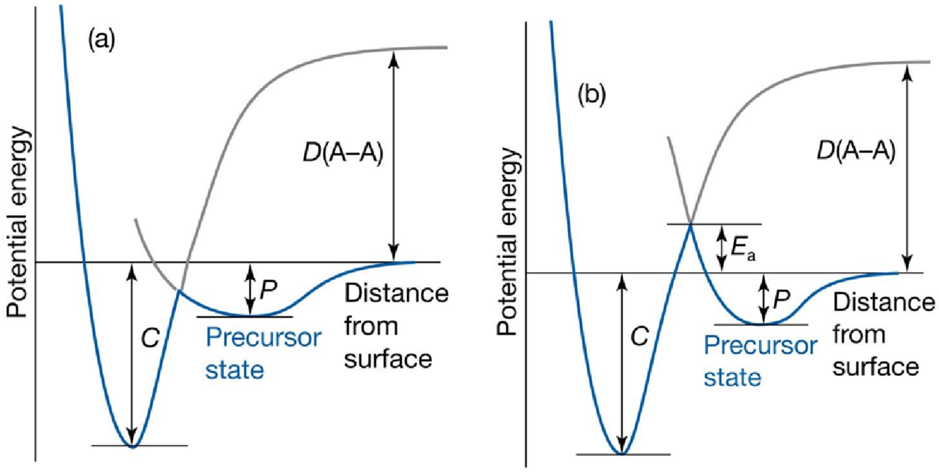

Not activated

Activated

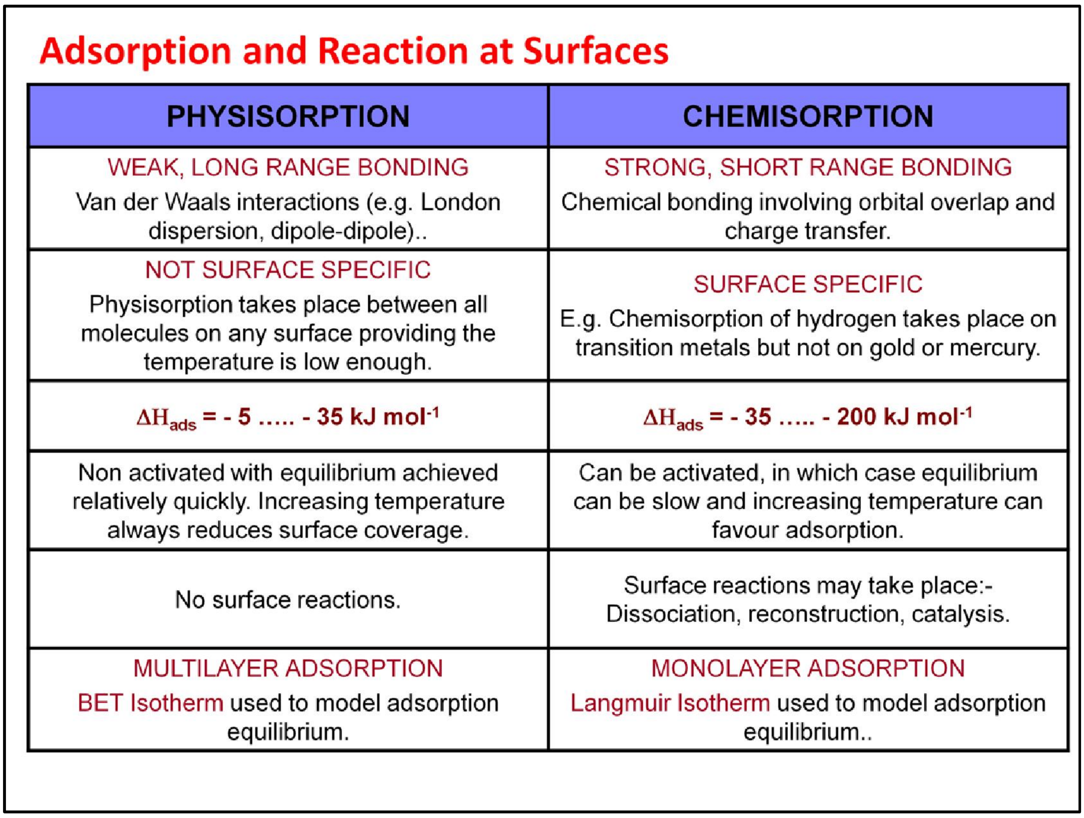

Adsorption and Reaction at Surfaces

PHYSISORPTION	CHEMISORPTION
WEAK, LONG RANGE BONDING Van der Waals interactions (e.g. London dispersion, dipole-dipole)..	STRONG, SHORT RANGE BONDING Chemical bonding involving orbital overlap and charge transfer.
NOT SURFACE SPECIFIC Physisorption takes place between all molecules on any surface providing the temperature is low enough.	SURFACE SPECIFIC E.g. Chemisorption of hydrogen takes place on transition metals but not on gold or mercury.
ΔH_{ads} = - 5 ….. - 35 kJ mol^{-1}	ΔH_{ads} = - 35 ….. - 200 kJ mol^{-1}
Non activated with equilibrium achieved relatively quickly. Increasing temperature always reduces surface coverage.	Can be activated, in which case equilibrium can be slow and increasing temperature can favour adsorption.
No surface reactions.	Surface reactions may take place:- Dissociation, reconstruction, catalysis.
MULTILAYER ADSORPTION BET Isotherm used to model adsorption equilibrium.	MONOLAYER ADSORPTION Langmuir Isotherm used to model adsorption equilibrium..

(1) Adsorption of CO on Metal Surfaces.

- orientation of the molecule
- coordinated to one, two or three metal atoms

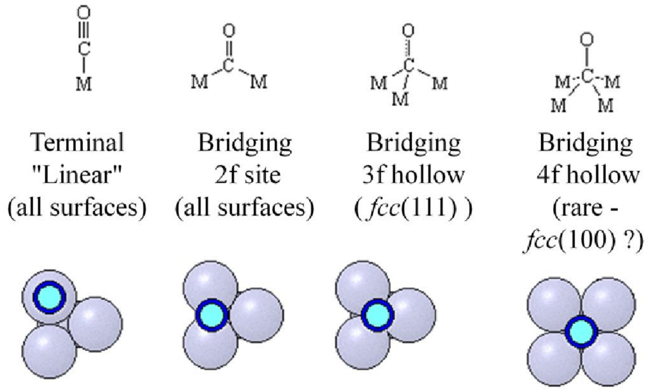

- interactions between the adsorbed CO molecules at high coverages.
- dissociation / temperature

(1) Adsorption of CO on Metal Surfaces.

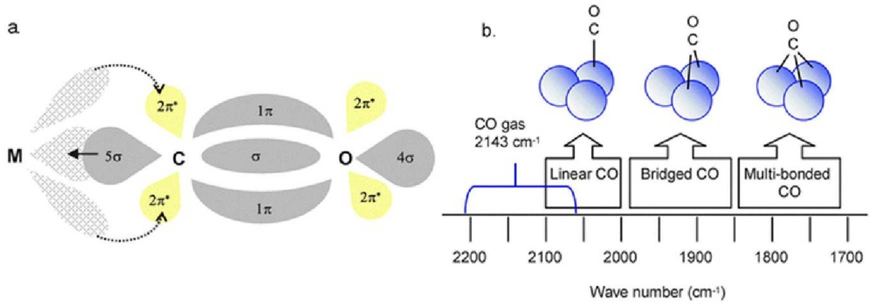

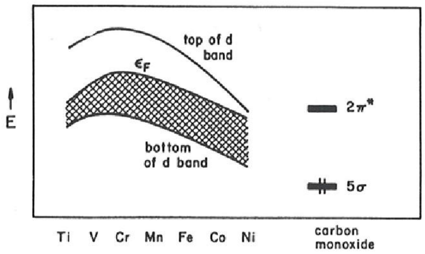

Figure 5.70 Superposition of the CO 5σ and $2\pi^*$ levels on the metal d band (see text). With permission from R. Hoffmann, *Solids and Surfaces: A Chemist's View of Bonding in Extended Surfaces.* VCH, Weinheim, 1988.

Dissociative adsorption

A. Hydrogen molecule approaching the W Surface end-on

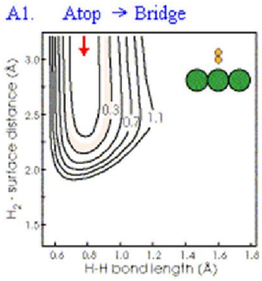
A1. Atop → Bridge

A1. When the hydrogen molecule approaches end-on to an atop site (i.e. from directly above a W atom) the potential energy increases rapidly for a molecule/surface separation of less than 2.3 Å. The molecule is therefore repelled from the surface.

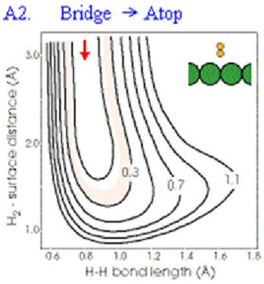
A2. Bridge → Atop

When the hydrogen molecule approaches end-on to a bridging site the potential energy increases slowly and although some lengthening of the H-H bond may occur with little corresponding increase in energy, there is no facile dissociation channel and the molecule is weakly repelled from the surface.

B. Hydrogen molecule approaching the W Surface broadside-on.

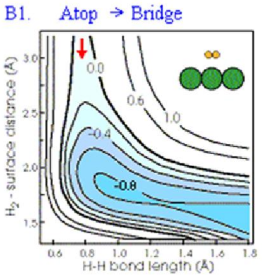

B1. When the hydrogen molecule approaches broadside-on to an atop site then the molecule may dissociate with considerable energy gain and there is no activation barrier to this process (i.e. the potential energy surface is strongly attractive). The deep well in the lower right corner corresponds to the hydrogen atoms produced by dissociation entering the bridge sites of the W surface.

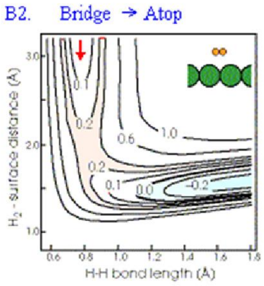

B2. When the hydrogen molecule approaches broadside-on to a bridge site then the molecule may again dissociate but the energy gain as the hydrogen atoms enter the atop sites is less marked than in the previous case (B1) and there is an activation barrier of ca. 0.2 eV that must be overcome for dissociation to occur.

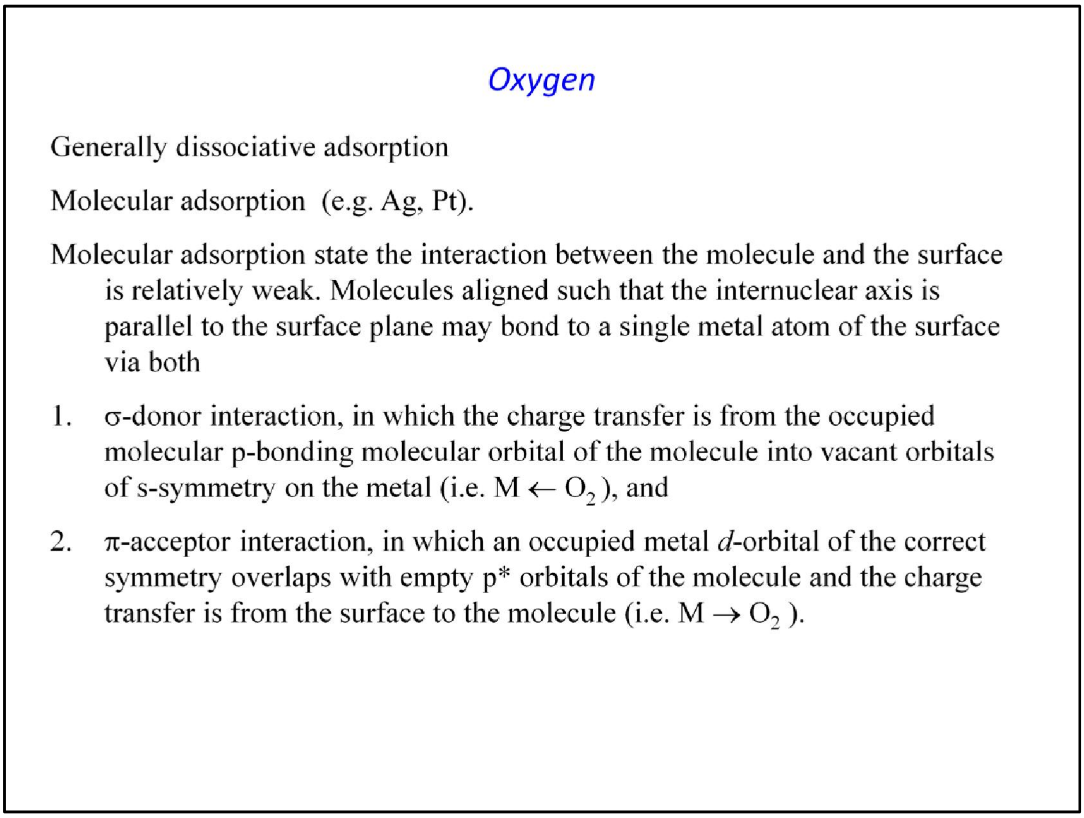

Oxygen

Generally dissociative adsorption

Molecular adsorption (e.g. Ag, Pt).

Molecular adsorption state the interaction between the molecule and the surface is relatively weak. Molecules aligned such that the internuclear axis is parallel to the surface plane may bond to a single metal atom of the surface via both

1. σ-donor interaction, in which the charge transfer is from the occupied molecular p-bonding molecular orbital of the molecule into vacant orbitals of s-symmetry on the metal (i.e. $M \leftarrow O_2$), and
2. π-acceptor interaction, in which an occupied metal *d*-orbital of the correct symmetry overlaps with empty p* orbitals of the molecule and the charge transfer is from the surface to the molecule (i.e. $M \rightarrow O_2$).

Although the interaction of the molecule with the surface is generally weak, one might expect that there might be a substantial barrier to dissociation due to the high strength (and high dissociation enthalpy) of the O=O bond. Nevertheless on most metal surfaces, dissociation of oxygen is observed to be facile which is related to the manner in which the interaction with the surface can mitigate the high intrinsic bond energy and thereby facilitate dissociation.

Once formed, oxygen atoms are strongly bound to the surface and, as noted previously, will tend to occupy the highest available co-ordination site. The strength of the interaction between adsorbate and substrate is such that the adjacent metal atoms are often seen to undergo significant displacements from the equilibrium positions that they occupy on the clean metal surface. This displacement may simply lead to a distortion of the substrate surface in the immediate vicinity of the adsorbed atom (so that, for example, the adjacent metal atoms are drawn in towards the oxygen and the metal-oxygen bond distance is reduced) or to a more extended surface reconstruction.

Chemisorption of Unsaturated Hydrocarbons

Unsaturated hydrocarbons (alkenes, alkynes, aromatic molecules etc.) all tend to interact fairly strongly with metal atom surfaces. At low temperatures (and on less reactive metal surfaces) the adsorption may be molecular, albeit perhaps with some distortion of bond angles around the carbon atom.

Ethene, for example, may bond to give both a π-complex (**A**) or a di-σ adsorption complex (**B**):

(**A**) *Chemisorbed Ethene* (**B**)

Models of chemisorbed ethene and ethyne on Cu(111)

Studies of ethylene (ethene) and acetylene (ethyne) chemisorbed on Cu(111), a surface with which they interact relatively weakly, have led to the following proposed structures for the molecular adsorption complexes.

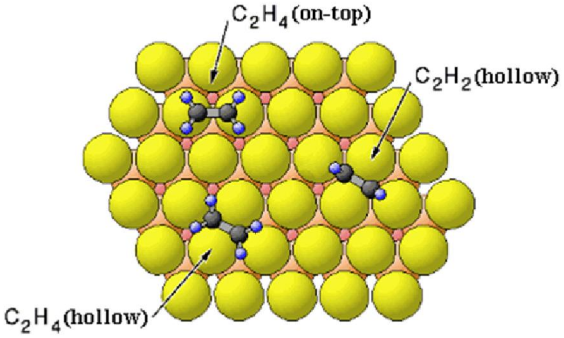

A. Plan view of the Cu(111) surface showing the adsorption geometry of athylene and acetylene molecules at low temperatures.

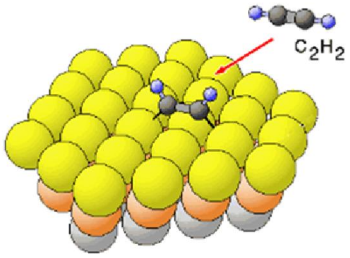

B. Perspective view of the Cu(111) surface with an adsorbed acetylene molecule, illustrating the re-hybridisation of the carbon centres to a geometry more closely associated with a C=C double-bond configuration.

Adsorption kinetics

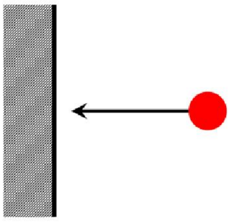

$$r_{ads} = kp^n$$ Macroscopic

$$r_{ads} = \frac{dN_{ads}}{dt} = F\,S$$ Microscopic

$$F = \frac{p}{(2\pi mkT)^{1/2}}$$

Probability of molecule being associatively adsorbed may defined in terms of a **sticking probability, S.**

$$S = \frac{\text{rate of adsorption of molecules by the surface}}{\text{rate of collison of molecules with the surface}}$$

$$S = S_0(1-\theta)^n = f_{(\theta)}exp\left({}^{-E_{ads}}/_{RT}\right) \qquad 0 < \theta < 1$$

$$\boxed{r_{ads} = \frac{dN_{ads}}{dt} = \frac{f_{(\theta)}\,p}{(2\pi mkT)^{1/2}}exp\left({}^{-E_{ads}}/_{RT}\right)}$$

Desorption kinetics

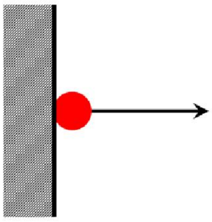

$$\boxed{r_{des} = -\frac{dN_{ads}}{dt} = A\, f'_{(\theta)}\, exp\left({}^{-E_{des}}/_{RT}\right)}$$

$$f'_{(\theta)} = \theta^n$$

$CO_{ads} \longrightarrow CO_{(g)}$ n = 1

$2\ O_{ads} \longrightarrow O_{2\ (g)}$ n = 2

Langmuir isotherm

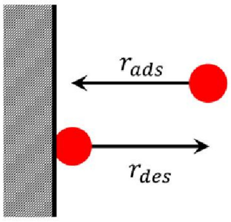

At the equilibrium:

$$r_{ads} = r_{des}$$

$$\frac{f_{(\theta)}\, p}{(2\pi mkT)^{1/2}}\, exp\left({}^{-E_{ads}}/_{RT}\right) = A\, f'_{(\theta)}\, exp\left({}^{-E_{des}}/_{RT}\right)$$

$$\frac{f_{(\theta)}\ p}{f'_{(\theta)}} = A\,(2\pi mkT)^{1/2} exp\left({}^{-\Delta H_{ads}}/_{RT}\right)$$

$$\Delta H_{ads} = E_{des} - E_{ads}$$

If:

- ΔH_{ads} does not depend from θ
- gas flow described by ideal gas law
- $\theta_{MAX} = 1$

$$\frac{f_{(\theta)}\ p}{f'_{(\theta)}} = C_{(T)}$$

Langmuir isotherm

Molecular chemisorption

$$\mathrm{S}-\square_{(s)} + \mathrm{A}_{(g)} \rightleftharpoons \mathrm{S}-\mathrm{A}_{(s)}$$

$$f_{(\theta)} = 1 - \theta \qquad\qquad f'_{(\theta)} = \theta$$

$$\frac{(1-\theta)\,p}{\theta} = C_{(T)} \quad \xRightarrow{C_{(T)} = {}^{1}\!/_{b}} \quad \theta = \frac{b\,p}{1+bp}$$

Dissociative chemisorption

$$2\,\mathrm{S}-\square_{(s)} + \mathrm{A}_{2\,(g)} \rightleftharpoons 2\,\mathrm{S}-\mathrm{A}_{(s)}$$

$$f_{(\theta)} = (1-\theta)^2 \qquad\qquad f'_{(\theta)} = \theta^{\,2}$$

$$\frac{(1-\theta)^2\,p}{\theta^{\,2}} = C_{(T)} \quad \xRightarrow{C_{(T)} = {}^{1}\!/_{b}} \quad \theta = \frac{(b\,p)^{1/2}}{1+(b\,p)^{1/2}}$$

General equation

$$\boxed{\theta = \frac{(b\,p)^{1/n}}{1+(b\,p)^{1/n}}}$$

Co-adsorption

Molecular chemisorption

$$\mathrm{S}-\square_{(s)} + \mathrm{A}_{(g)} \rightleftharpoons \mathrm{S}-\mathrm{A}_{(s)}$$

$$\mathrm{S}-\square_{(s)} + \mathrm{B}_{(g)} \rightleftharpoons \mathrm{S}-\mathrm{B}_{(s)}$$

$$\theta_A = \frac{b_A p_A}{1 + b_A p_A + b_B p_B} \qquad \theta_B = \frac{b_B p_B}{1 + b_A p_A + b_B p_B}$$

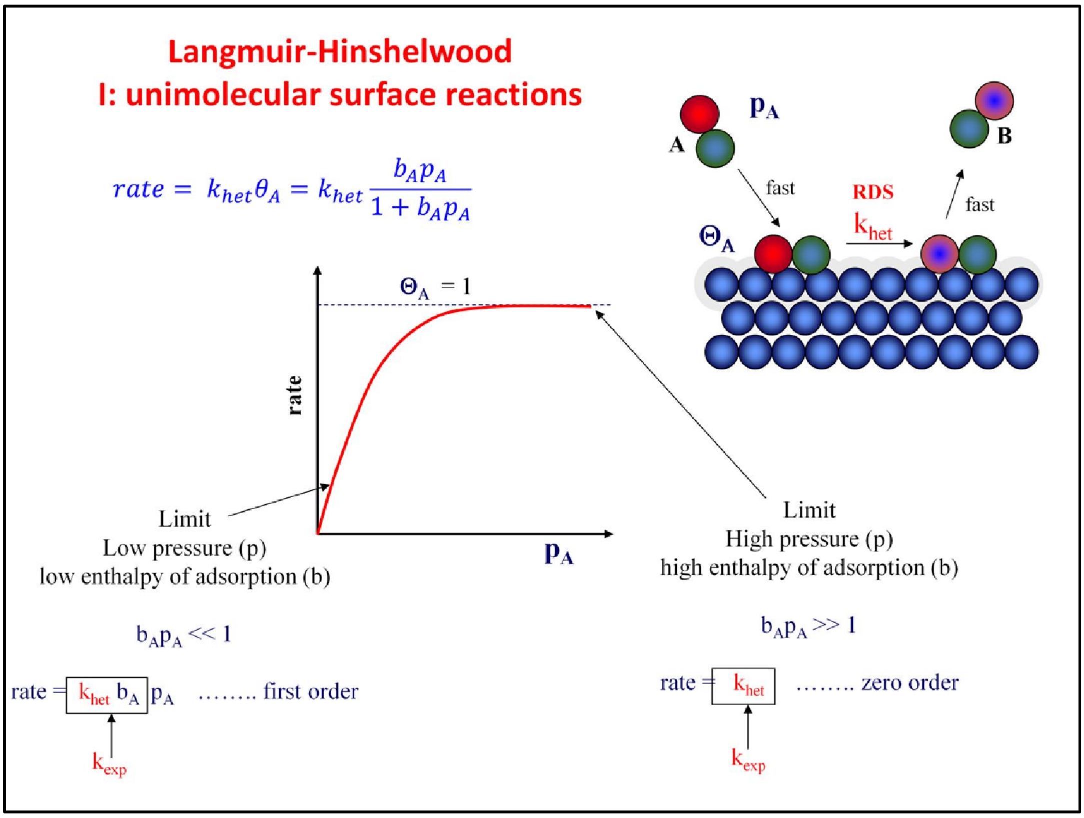

Langmuir-Hinshelwood
I: unimolecular surface reactions

$$rate = k_{het}\theta_A = k_{het}\frac{b_Ap_A}{1+b_Ap_A}$$

Limit
Low pressure (p)
low enthalpy of adsorption (b)

$b_Ap_A \ll 1$

rate = $\boxed{k_{het}\, b_A}\, p_A$ …….. first order

k_{exp}

Limit
High pressure (p)
high enthalpy of adsorption (b)

$b_Ap_A \gg 1$

rate = $\boxed{k_{het}}$ …….. zero order

k_{exp}

Langmuir-Hinshelwood
II: bimolecular surface reactions

$$rate = k_{het}\,\theta_A\theta_B = k_{het}\frac{b_A p_A b_B p_B}{(1 + b_A p_A + b_B p_B)^2}$$

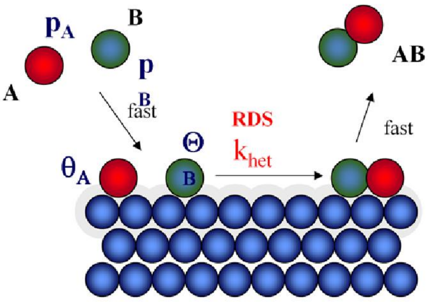

Langmuir-Hinshelwood
II: bimolecular surface reactions

$$rate = k_{het}\,\theta_A\theta_B = k_{het}\frac{b_A p_A b_B p_B}{(1 + b_A p_A + b_B p_B)^2}$$

$$\boxed{b_A \sim b_B}$$

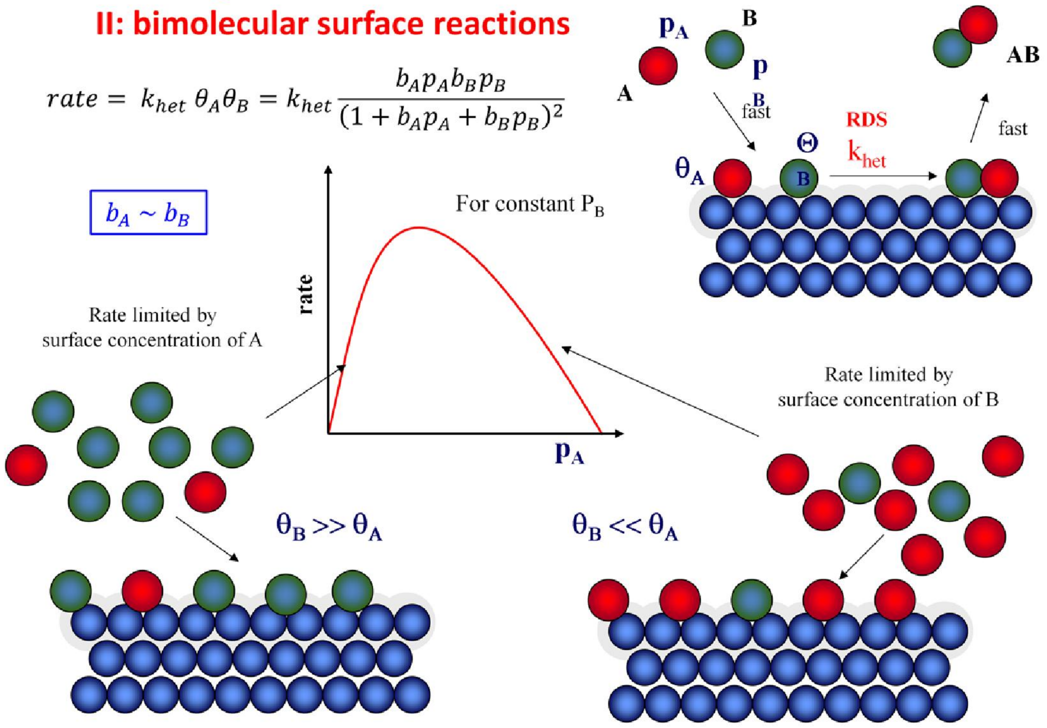

Langmuir-Hinshelwood
II: bimolecular surface reactions

$$rate = k_{het}\,\theta_A\theta_B = k_{het}\frac{b_A p_A b_B p_B}{(1 + b_A p_A + b_B p_B)^2}$$

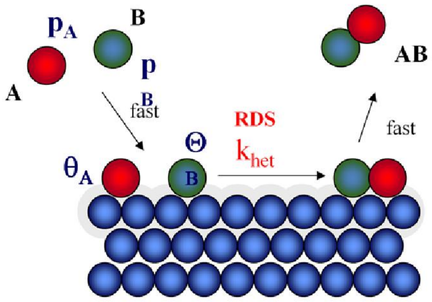

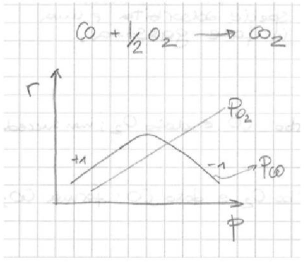

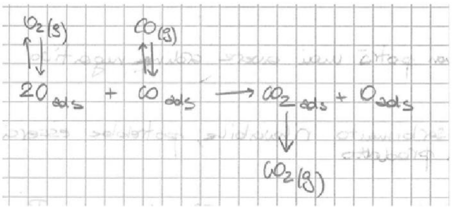

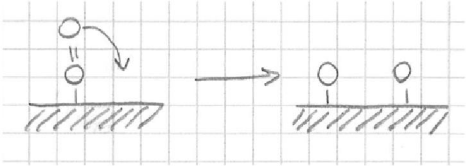

O_2 needs 2 sites to dissociate and react. As p_{CO} increases, the number of adjacent sites decreases, reducing the rate of the reaction.

Langmuir-Hinshelwood
II: bimolecular surface reactions

$$rate = k_{het}\,\theta_A\theta_B = k_{het}\frac{b_Ap_Ab_Bp_B}{(1+b_Ap_A+b_Bp_B)^2}$$

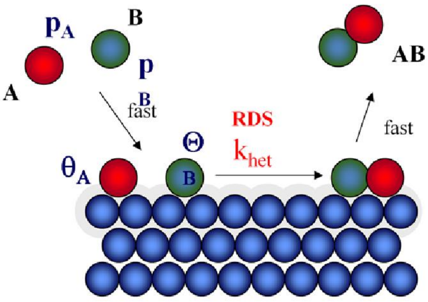

$$\boxed{b_A \ll b_B}$$

$$b_Bp_B \gg b_Ap_A + 1$$

$$rate = k_{het}\frac{b_Ap_A}{b_Bp_B}$$

B has a negative reaction order.

B acts as a POISON of the reaction

Eley-Rideal bimolecular surface reactions

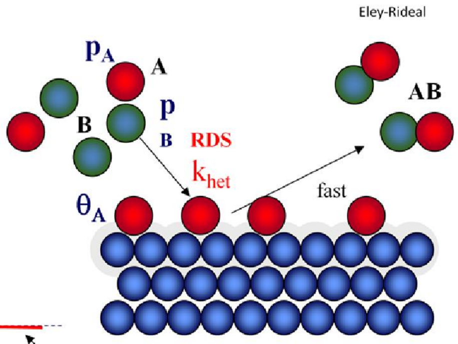

An adsorbed molecule may react directly with an impinging gas molecule by a collisional mechanism

$$rate = k_{het}\,\theta_A p_B = k_{het} p_B \frac{b_A p_A}{1 + b_A p_A}$$

Note: For constant p_A, the rate is always first order wrt $\mathbf{p_B}$

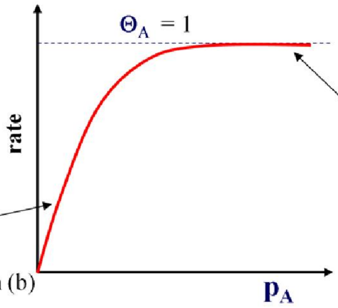

Limit
Low pressure (p)
low enthalpy of adsorption (b)

$b_A p_A \ll 1$

$$rate = \underbrace{\boxed{k_{het}\, b_A}}_{k_{exp}}\; p_A\, \mathbf{p_B} \text{ …….. first order in A}$$

Limit
High pressure (p)
high enthalpy of adsorption (b)

$b_A p_A \gg 1$

$$rate = \underbrace{\boxed{k_{het}}}_{k_{exp}}\; \mathbf{p_B} \text{ …….. zero order in A}$$

Transition State Model and Catalyst Activity
The Volcano Plot

There is often a relationship between CATALYTIC ACTIVITY (ΔE_{het}) and strength of chemisorption of reactants ΔH_{ads}.

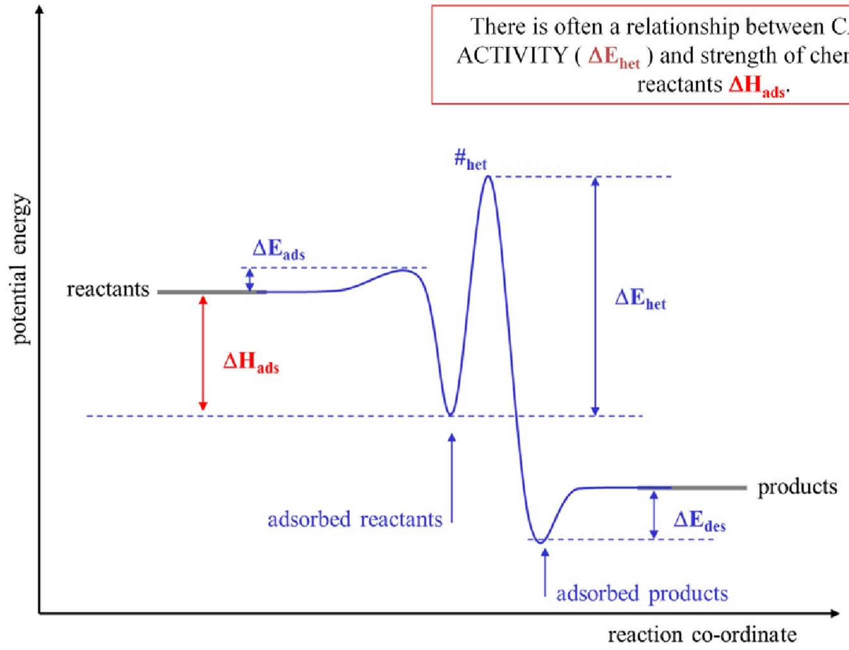

The Volcano Plot

Rootsaert & Sachtler: Z.Phys.Chem. 26 (1960) 16

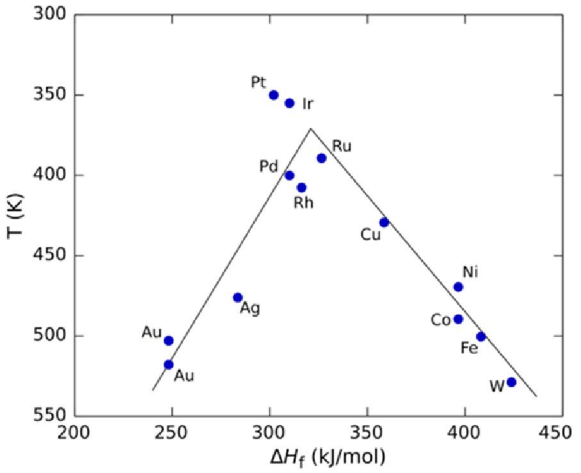

$HCCOH \longrightarrow CO_2 + H_2$

When $-\Delta H_{ads}$ is small
bp << 1
Θ = bp α exp ($-\Delta G_{ads}/RT$) α exp ($-\Delta H_{ads}/RT$)
Increasing $-\Delta H_{ads}$ **will increase Θ and hence rate.**
ΔE_{het} remains unchanged.

When $-\Delta H_{ads}$ is large
bp >> 1, and **Θ = 1**
Increasing $-\Delta H_{ads}$ **starts to increase ΔE_{het} and rate decreases (adsorbates too stable to react.**

Transition State Model and Catalyst Activity
The Volcano Plot

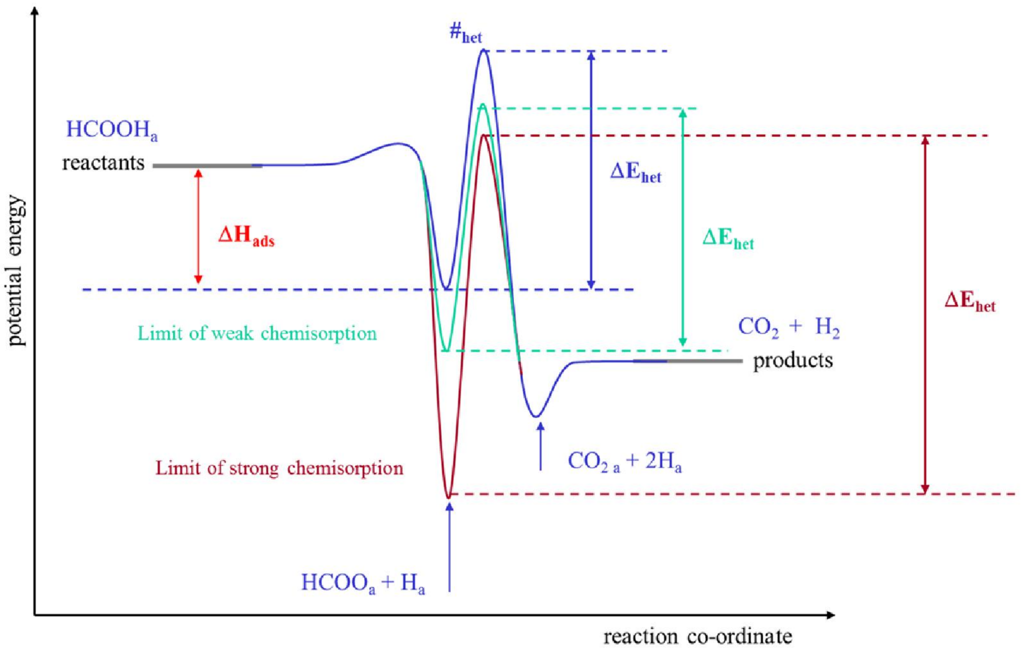

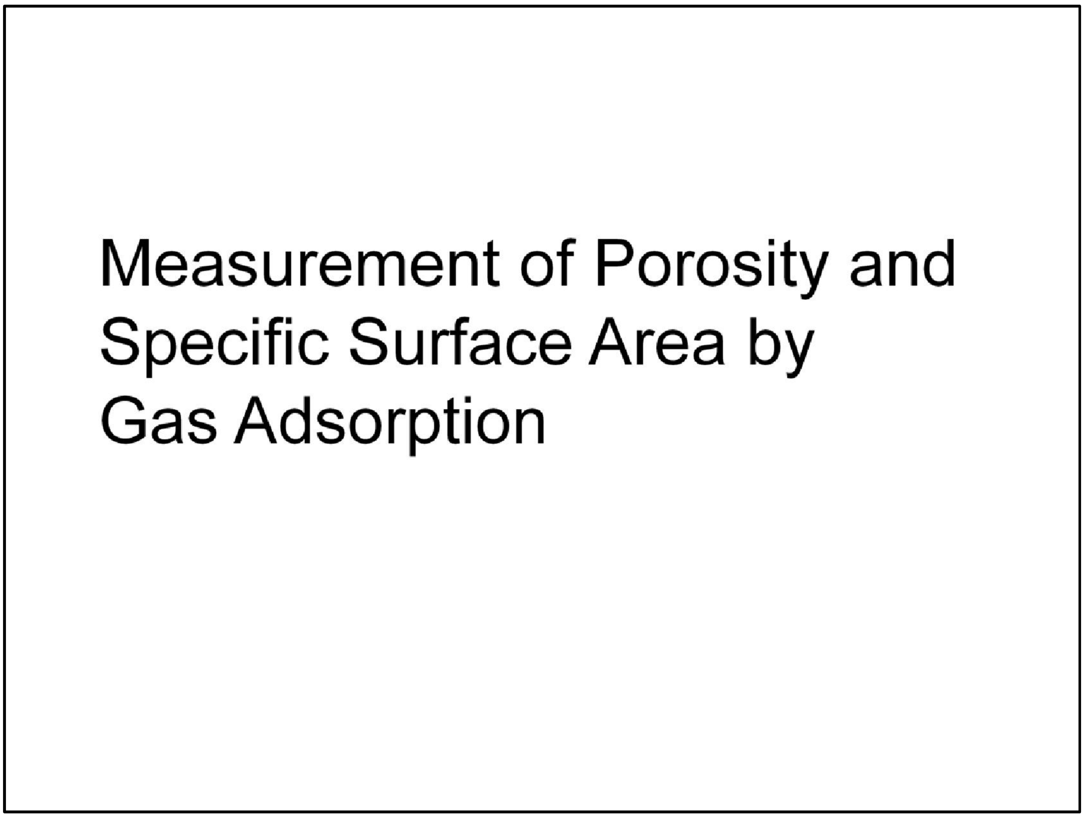

Measurement of Porosity and Specific Surface Area by Gas Adsorption

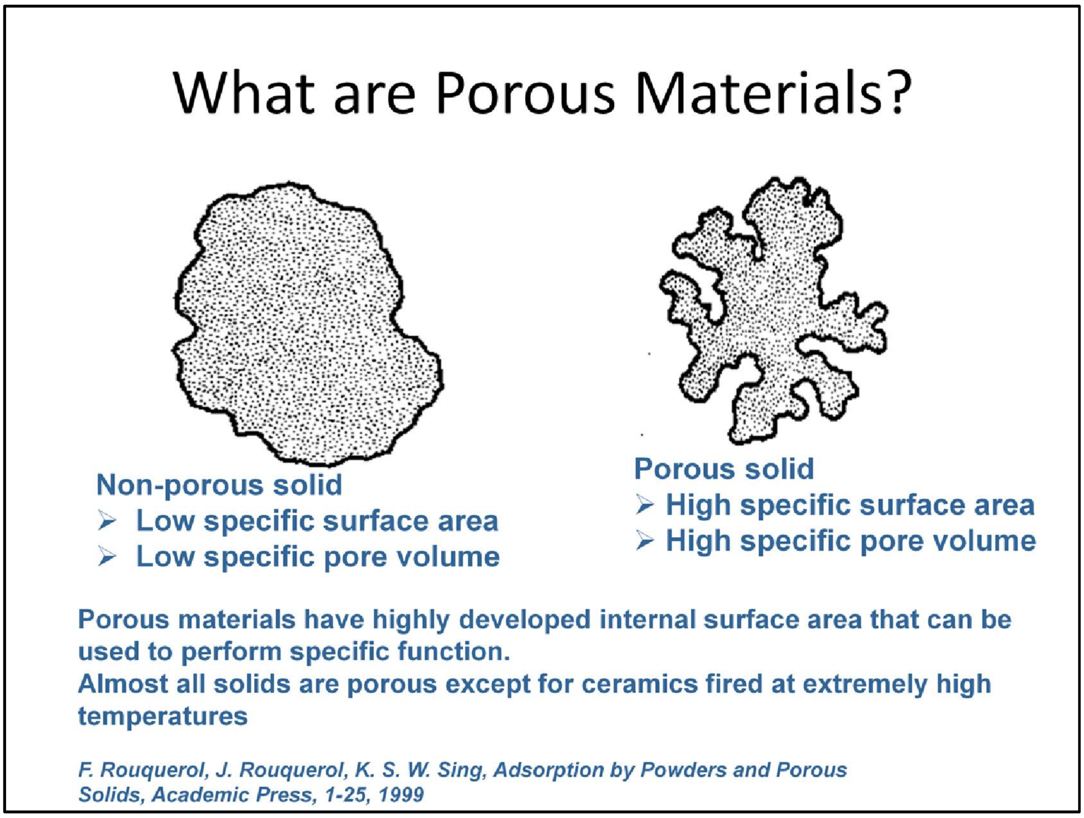

What are Porous Materials?

Non-porous solid

- **Low specific surface area**
- **Low specific pore volume**

Porous solid

- **High specific surface area**
- **High specific pore volume**

Porous materials have highly developed internal surface area that can be used to perform specific function.
Almost all solids are porous except for ceramics fired at extremely high temperatures

F. Rouquerol, J. Rouquerol, K. S. W. Sing, Adsorption by Powders and Porous Solids, Academic Press, 1-25, 1999

All solids can be classified in to two categories; porous and non-porous solids. Porous solids are those that have high surface area and high pore volume where as non-porous solids are those that have low surface area and low pore volume. In general, all solids to some extend are porous except ceramics fired at high temperatures.

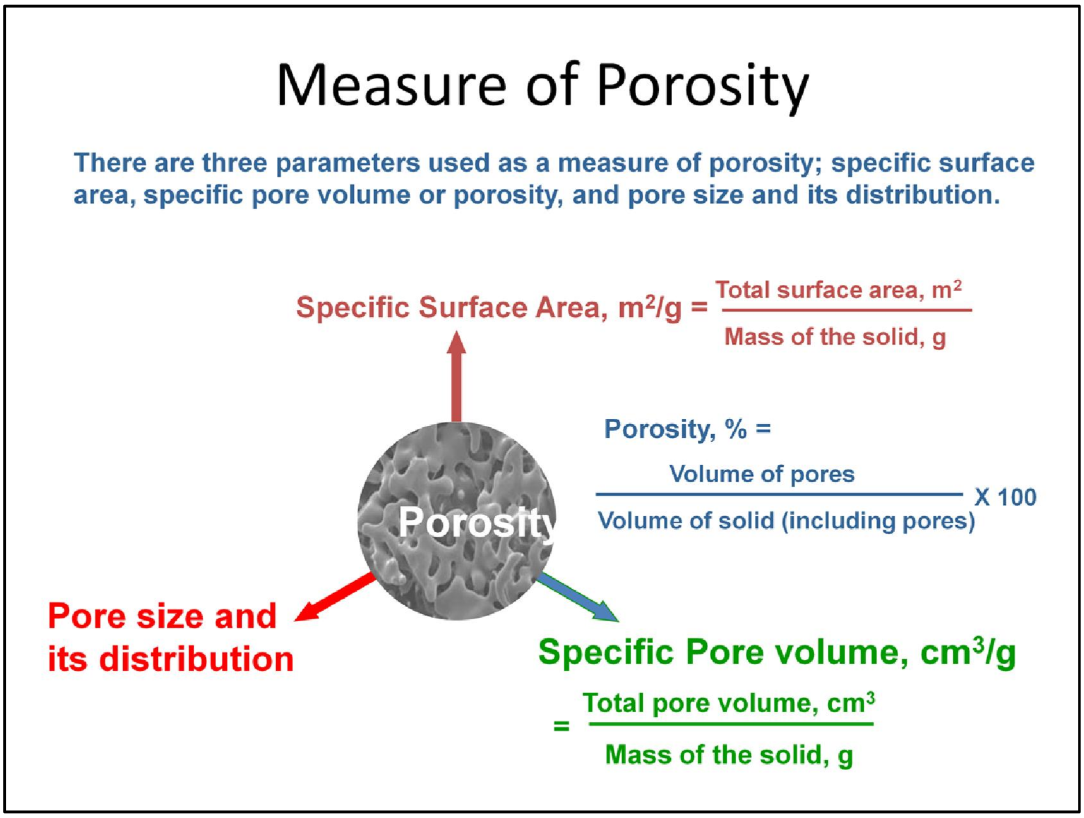

Measure of Porosity

There are three parameters used as a measure of porosity; specific surface area, specific pore volume or porosity, and pore size and its distribution.

Specific Surface Area, $m^2/g = \dfrac{\text{Total surface area, } m^2}{\text{Mass of the solid, g}}$

Porosity

Porosity, % = $\dfrac{\text{Volume of pores}}{\text{Volume of solid (including pores)}} \times 100$

Pore size and its distribution

Specific Pore volume, cm^3/g

$= \dfrac{\text{Total pore volume, } cm^3}{\text{Mass of the solid, g}}$

The three measure of a porous solids are surface area, pore size and its distribution and pore volume.

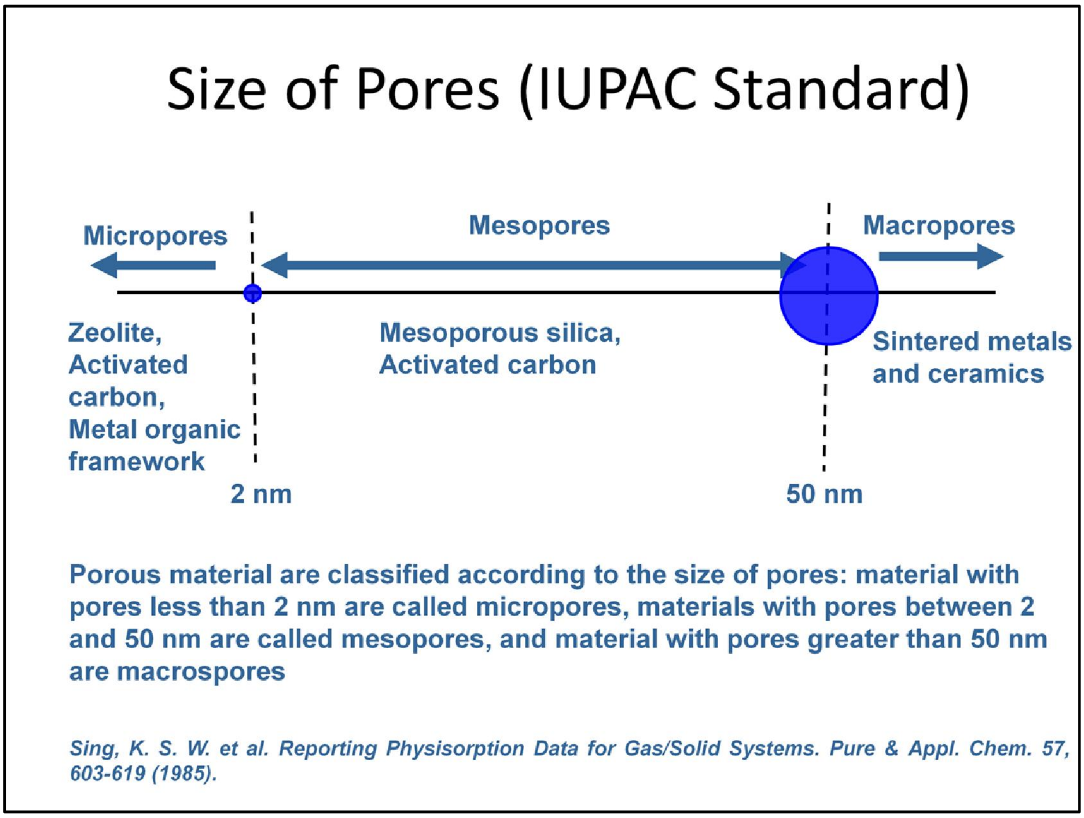

Size of Pores (IUPAC Standard)

Porous material are classified according to the size of pores: material with pores less than 2 nm are called micropores, materials with pores between 2 and 50 nm are called mesopores, and material with pores greater than 50 nm are macrospores

Sing, K. S. W. et al. Reporting Physisorption Data for Gas/Solid Systems. Pure & Appl. Chem. 57, 603-619 (1985).

Pores can be open or closed. Open pores are accessible where as closed pores are inaccessible. Open pores

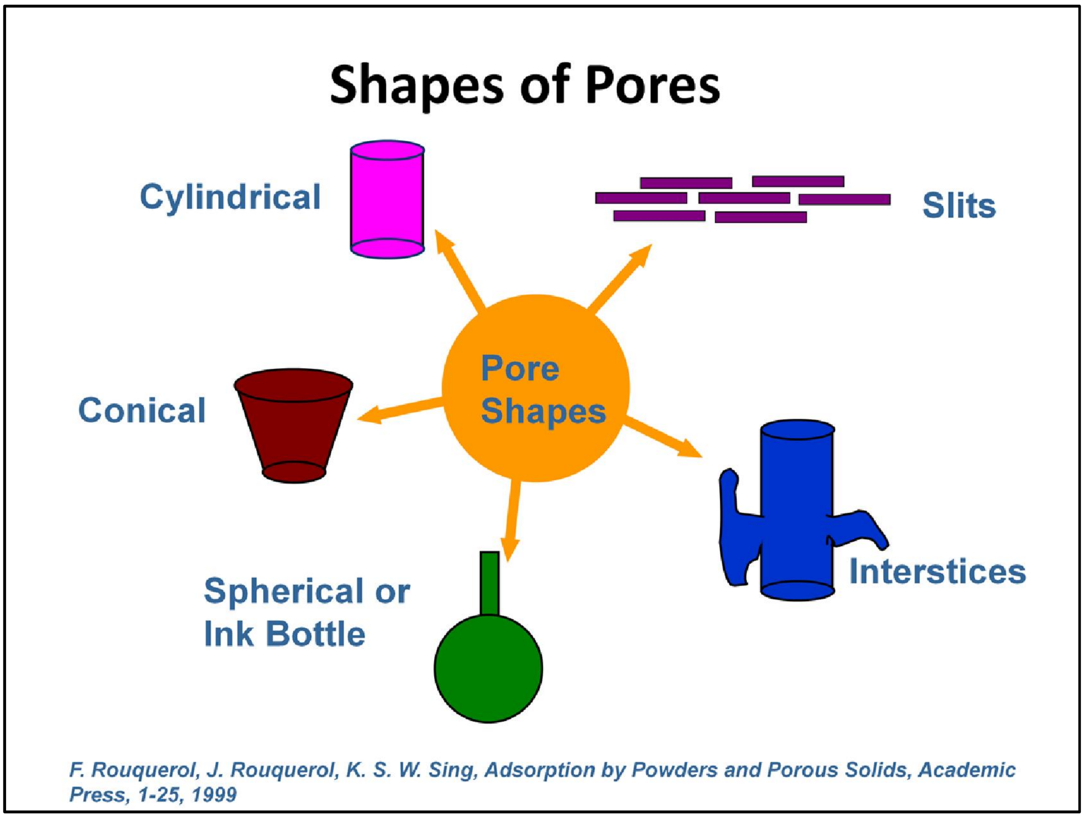

Shapes of Pores

Pore Shapes

Cylindrical

Slits

Conical

Interstices

Spherical or
Ink Bottle

F. Rouquerol, J. Rouquerol, K. S. W. Sing, Adsorption by Powders and Porous Solids, Academic Press, 1-25, 1999

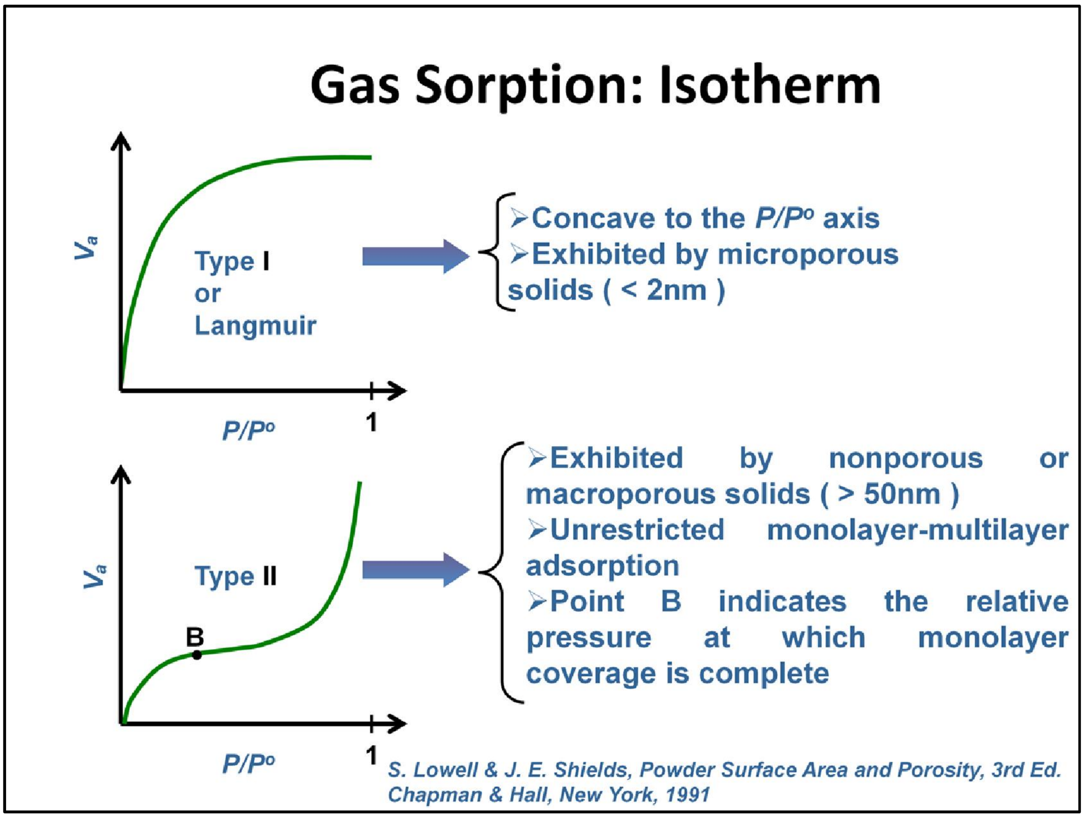

Gas Sorption: Isotherm

- Concave to the P/P^o axis
- Exhibited by microporous solids (< 2nm)

- Exhibited by nonporous or macroporous solids (> 50nm)
- Unrestricted monolayer-multilayer adsorption
- Point B indicates the relative pressure at which monolayer coverage is complete

S. Lowell & J. E. Shields, Powder Surface Area and Porosity, 3rd Ed. Chapman & Hall, New York, 1991

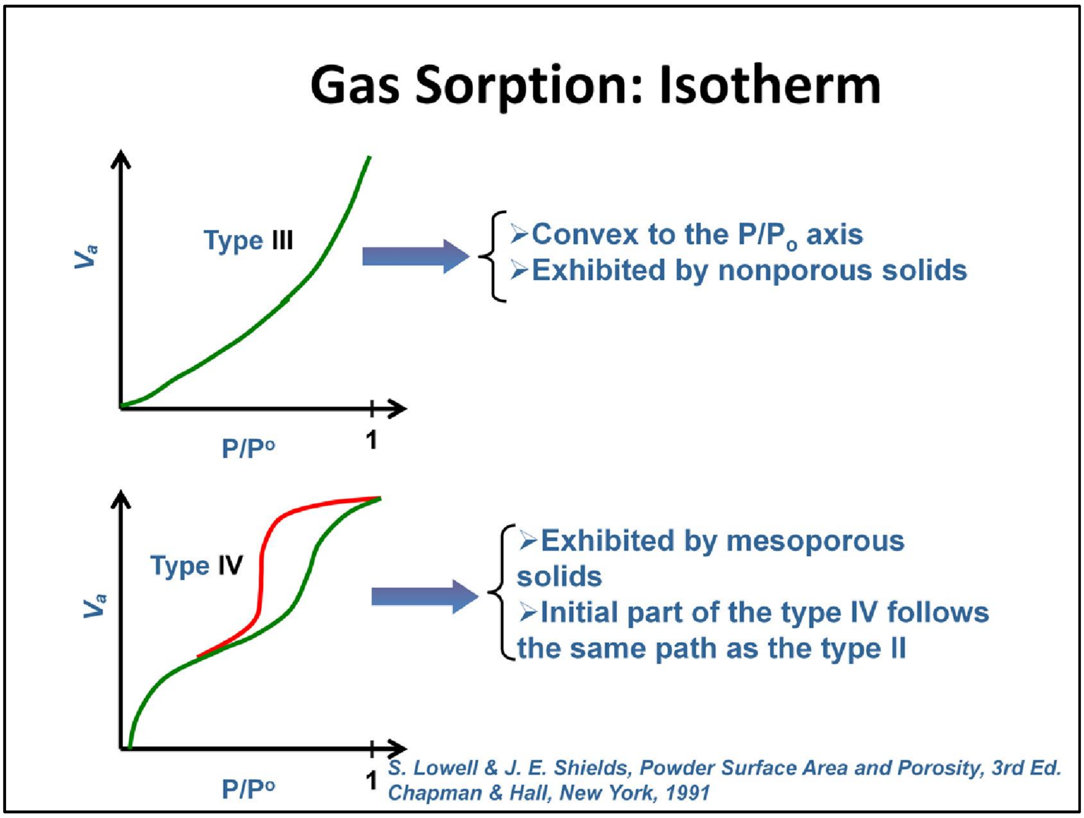

Gas Sorption: Isotherm

- ➢Convex to the P/P_o axis
- ➢Exhibited by nonporous solids

- ➢Exhibited by mesoporous solids
- ➢Initial part of the type IV follows the same path as the type II

S. Lowell & J. E. Shields, Powder Surface Area and Porosity, 3rd Ed. Chapman & Hall, New York, 1991

Gas Sorption: Isotherm

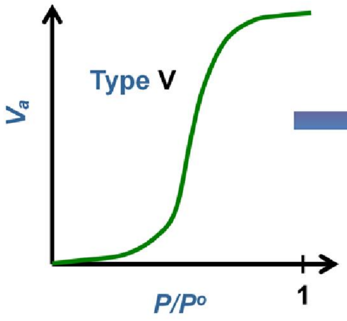

- ➢Highly uncommon
- ➢Exhibited by mesoporous solids

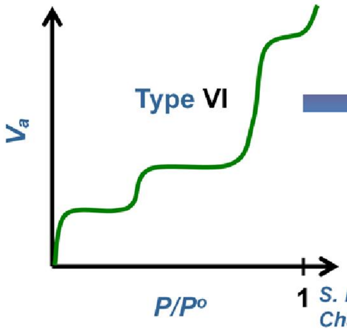

- ➢Exhibited by nonporous solids with an almost completely uniform surface

S. Lowell & J. E. Shields, Powder Surface Area and Porosity, 3rd Ed. Chapman & Hall, New York, 1991

Gas Sorption: Hysteresis

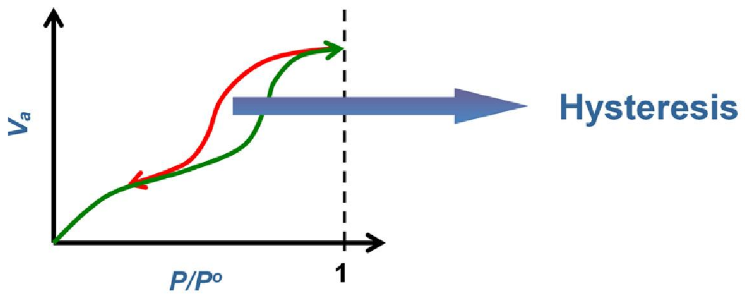

- ➢Hysteresis indicates the presence of mesopores.
- ➢Hysteresis gives information regarding pore shapes .
- ➢Types I, II and III isotherms are generally reversible but type I can have a hysteresis. Types IV and V exhibit hysteresis.

S. Lowell & J. E. Shields, Powder Surface Area and Porosity, 3rd Ed.
Chapman & Hall, New York, 1991

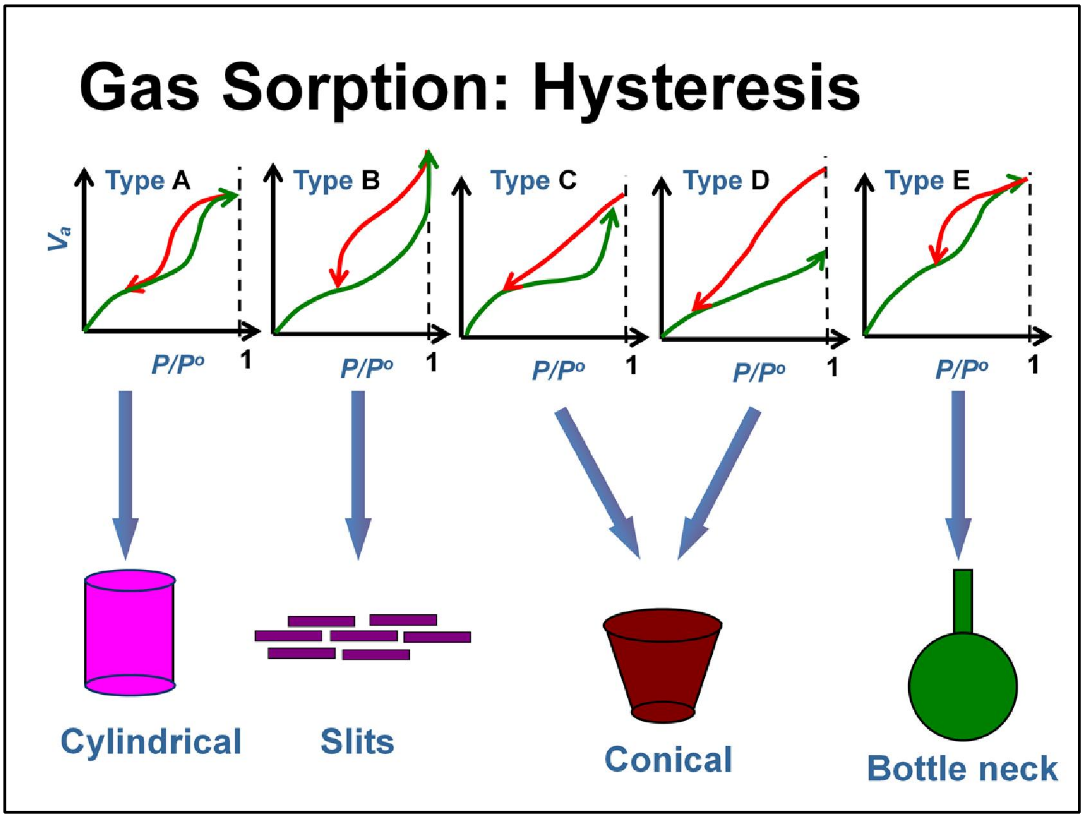

Gas Sorption: Hysteresis

Adsorption Theories: BET

$$\frac{P}{V_a(P-P^o)} = \frac{1}{V_mC} + \frac{(C-1)}{V_mC}\left(\frac{P}{P^o}\right)$$

S.Brunauer, P.Emmett, E.Teller Adsorption of Gases in Multimolecular Layers, J. Am. Chem. Soc., 1938, 60 (2), pp 309–319

where

V_a = volume of gas adsorbed at pressure P;

V_m = volume of gas required to form monolayer;

C = BET constant (related to energy of adsorption of 1st layer); and

$\frac{P}{P^o}$ = relative pressure of adsorbate.

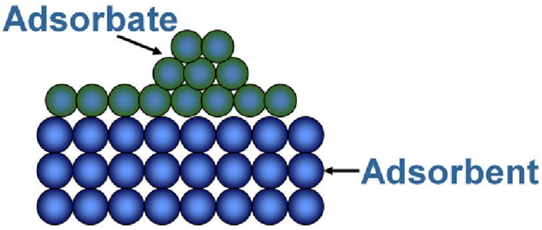

- **Modification of Langmuir isotherm**
- **Both monolayer and multilayer adsorption**
- **Assumptions:**

(a) **gas molecules physically adsorb on a solid in layers infinitely;**

(b) **there is no interaction between each adsorption layer;**

(c) **the Langmuir theory can be applied to each layer.**

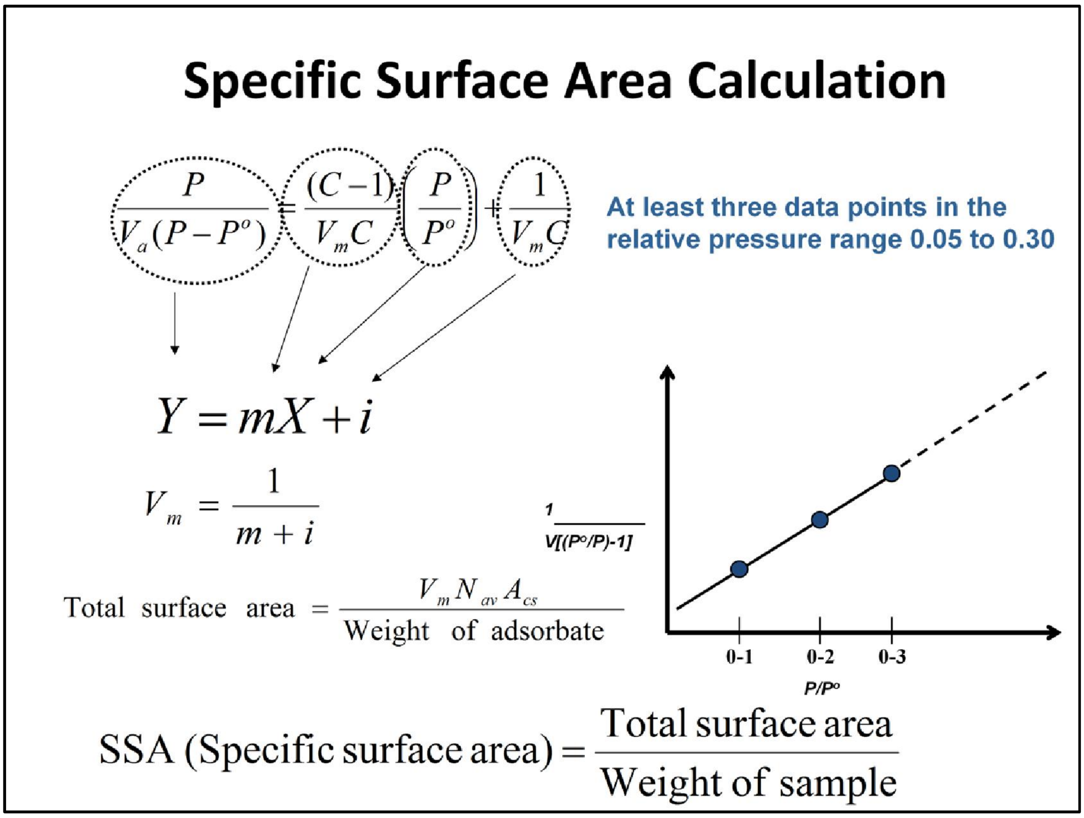

Specific Surface Area Calculation

$$\underbrace{\frac{P}{V_a(P-P^o)}}_{Y}=\underbrace{\frac{(C-1)}{V_mC}}_{m}\underbrace{\left(\frac{P}{P^o}\right)}_{X}+\underbrace{\frac{1}{V_mC}}_{i}$$

At least three data points in the relative pressure range 0.05 to 0.30

$$Y=mX+i$$

$$V_m=\frac{1}{m+i}$$

$$\text{Total surface area}=\frac{V_mN_{av}A_{cs}}{\text{Weight of adsorbate}}$$

$$\text{SSA (Specific surface area)}=\frac{\text{Total surface area}}{\text{Weight of sample}}$$

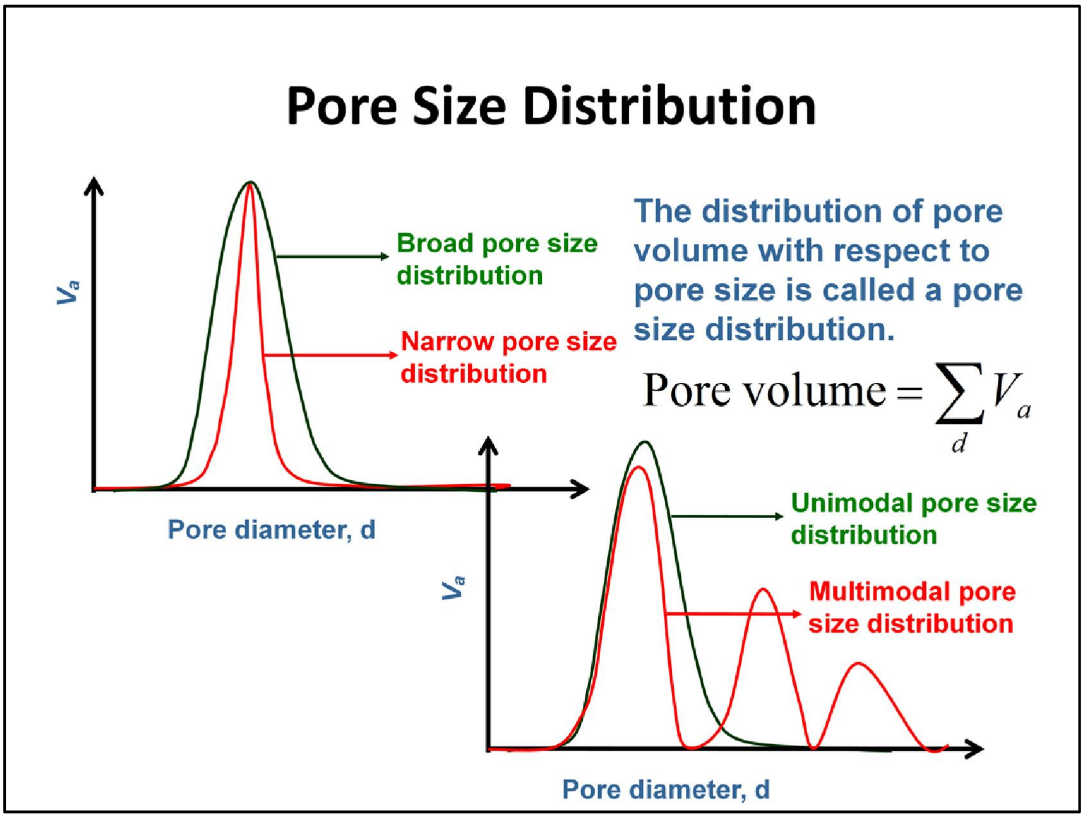

Pore Size Distribution

The distribution of pore volume with respect to pore size is called a pore size distribution.

$$\text{Pore volume} = \sum_{d} V_a$$

Pore Size Distribution

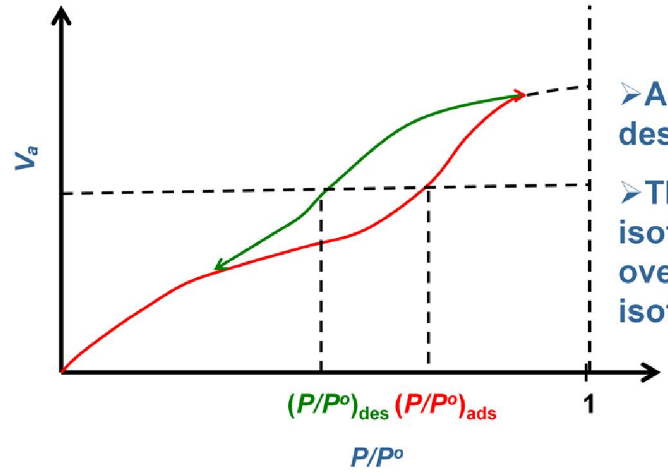

- Adsorption or desorption isotherm.
- The desorption isotherm is preferred over adsorption isotherm.

$$\left\{\begin{aligned} \Delta G_{des} &= RT(\ln P_{des} - \ln P^0) \\ \Delta G_{ads} &= RT(\ln P_{ads} - \ln P^0) \end{aligned}\right\} \quad \boxed{\Delta G_{des} < \Delta G_{ads}}$$

Pore Size: Kelvin Equation

$$\ln\left(\frac{p}{p^{o}}\right) = \frac{2\gamma V}{r_k RT}\cos\theta$$

where

$$\left(\frac{p}{p^{o}}\right) = \left(\frac{\text{pressure of adsorbate}}{\text{saturated pressure of adsorbate}}\right);$$

γ = liquid surface tension;

V = molar volume of condensed adsorbate;

r_k = mean radius of curvature of the liquid meniscus;

R = real gas constant;

T = temperature;

θ = contact angle between the solid and condensed phase.

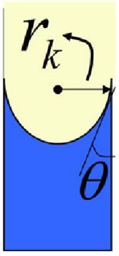

- Multilayer formation occurs in parallel to capillary condensation.
- Capillary condensation is described by the Kelvin equation.

Pore Size: Kelvin Equation

Prior to condensation, some adsorption has taken place on the walls of the pore, r_k does not represent the actual pore radius.

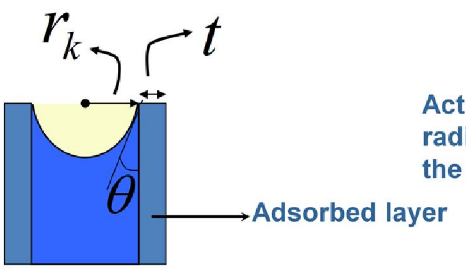

$$r_p = r_k + t$$

r_p → Actual radius of the pore

r_k → Kelvin radius of the pore

t → Thickness of the adsorbed layer

Isoterma di chemiadsorbimento

Il numero di atomi di metallo superficiale $N_{(s)M}$ e la superficie attiva del metallo S_M

$$N_{(s)M} = n \frac{\nu}{V_m} N_a$$

$$S_M = N_{(s)M}\, s$$

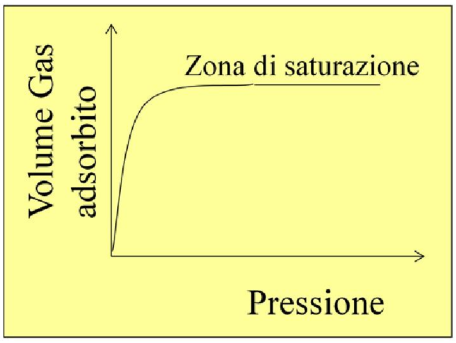

ν è il volume di gas adsorbito,
V_m il volume molare del gas,
s la superficie occupata da un atomo metallico,
n numero di atomi di metallo necessari per adsorbire una molecola di idrogeno
N_a il numero di Avogadro.

Stechiometria di chemiadsorbimento

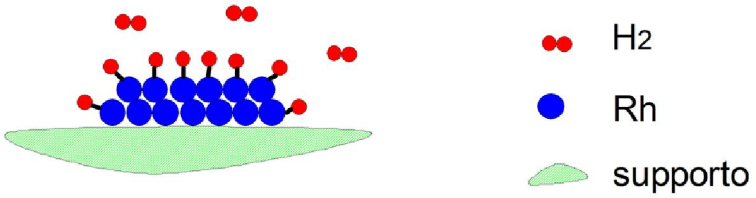

Rh : H = 1 : 1 n = 2

Diametro < 1 nm → n < 2

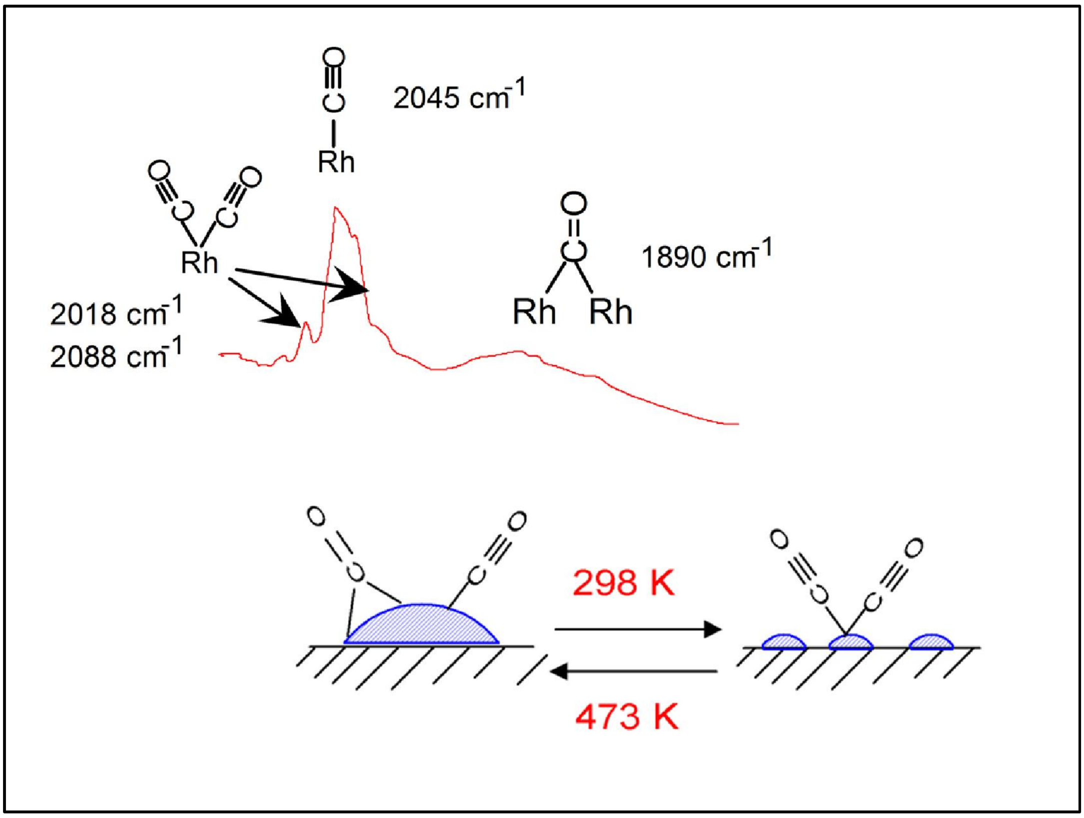
2045 cm^{-1}
Rh
Rh
2018 cm^{-1}
2088 cm^{-1}
1890 cm^{-1}
Rh
Rh
298 K
473 K

1.1% Pt/γ-Al_2O_3

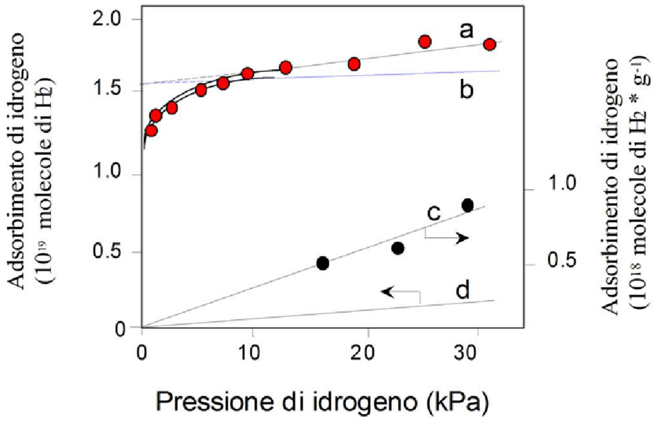

Adsorbimento a 573 K di H_2. Curva (a) adsorbimento su 2.031 g di catalizzatore, (c) adsorbimento su 1.00 g di Al_2O_3, (d) adsorbimento su quantità di supporto corrispondente a quella del campione (2.00 g) ed espressa nella stessa scala della curva (a), (b) differenza tra la curva a e d.

Dispersione metallica

$$D_M = \frac{N_{(s)M}}{N_{(tot)M}}$$

$N_{(s)M}$ numero di atomi superficiali di metallo

$N_{(tot)M}$ numero totale di atomi di metallo.

Diametro medio delle particelle metalliche (geometria sferica)

$$d_M = 6\frac{\sum_i V_i}{\sum_i A_i} = 6\frac{V_M}{a_M}\frac{N_{(tot)M}}{N_{(s)M}} = 6\frac{V_M}{a_M}\frac{1}{D_M}$$

$= 6\ V/A$

a_M l'area media occupata da un atomo di metallo

V_M è il volume di un atomo di metallo nel "bulk".

$$V_M = \frac{M_w}{\rho N_a}$$

M_w peso atomico del metallo, ρ la sua densità N_a numero di Avogadro.

Important industrial processes

Process	Products
Reforming	Syn-gas (H_2+CO+CO_2) from HC
Water Gas Shift	H_2 purification
Haber- Bosch	Ammonia synthesis
Fisher-Tropsch	Synthetic fuel from syn-gas
Methanol	Methanol from syn-gas
MTO	Olefins from methanol
HDS & HDN	Fuel purification
Hydrogenation	Fuel upgrading
Hydrocacking	Fuel upgrading
TWC	Exhaust purification

Ammonia synthesis

$$3\,\mathrm{H_2(g)} + \mathrm{N_2(g)} \rightleftharpoons 2\,\mathrm{NH_3} \qquad -\Delta H_{773\mathrm{K}} = 109\,\mathrm{kJ\,mol^{-1}}$$

Haber-Bosch process
T = 450°C, P = 100-300bar

Catalysts: BASF-S6-10
$Fe_3O_4 + Al_2O_3 + CaO + K_2O$

Under reaction conditions, Fe_3O_4 is reduced to Fe.
Al_2O_3 and CaO have a structural effect, maintaining the surface area.
K_2O has an electronic effect lowering E_{att}.

$$\frac{\mathrm{d}p_{\mathrm{NH_3}}}{\mathrm{d}t} = k p_{\mathrm{N_2}} \left[\frac{p^3{}_{\mathrm{H_2}}}{p^2{}_{\mathrm{NH_3}}} \right]^i$$

i = 0.50 - 0.67

Ammonia synthesis

Surface composition of the catalyst

Table 8.3 Composition [atom%] of a promoted iron catalyst in per cent (after G. Ertl, D. Brigge, R. Schlögl, M. Weiss, *J. Catal.*, **1983**, *79*, 359).

	Fe	K	Al	Ca	O
Bulk composition	40.5	0.35	2.0	1.7	53.2
AES					
Before reduction	8.6	36.1	10.7	4.7	40.0
After reduction	11.0	27.0	17.0	4.0	41.0

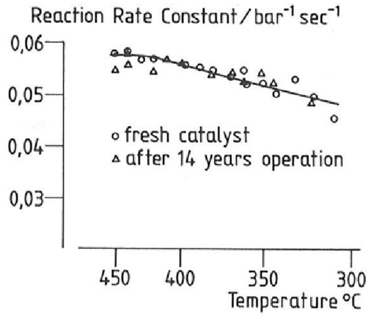

Extreme stability of the catalyst

At the operative temperature, the catalyst is in a “quasi liquid” form, allowing constant regeneration of the surface.

Ammonia synthesis

Atomic or molecular route?

$N_2(ad) + 6\,H(ad) \rightarrow 2\,NH_3$ (molecular route)

$N(ad) + 3\,H(ad) \rightarrow NH_3$ (atomic route)

$H_2 \overset{K_1}{\rightleftharpoons} 2H_a$ $T_{des} < 200\,°C$

$N_2 \overset{K_2}{\rightleftharpoons} N_2(ad)$ $T_{des} < -100\,°C$

$N_2(ad) \overset{K_3}{\rightleftharpoons} 2N(ad)$ $T_{des}\ 450\,°C$

$NH_3 \rightleftharpoons NH_3(ad)$ $T_{des} < 100\,°C$

It is possible to measure $N_{(ad)}$

Ammonia synthesis

Molecular route:
the surface would necessarily be saturated with $N_{(ad)}$ under steady-state conditions, since there would exist no channel through which this species could be removed.

Atomic route:
The steady-state concentration of $N_{(ad)}$ is:

$$\begin{aligned}\frac{d[N(ad)]}{dt} &= 0 = k_3[N_2(ad)] - k_0[N(ad)][H(ad)]^r \\ &= k_3 k_2 p_{N_2} - k_0 K_1 [N(ad)] p_{H_2}^q\end{aligned}$$

$$[N(ad)]_{stat} = k\frac{p_{N_2}}{p_{H_2}^q}$$

$N_{(ad)}$ should decrease as p_{H2} increases.

Ammonia synthesis

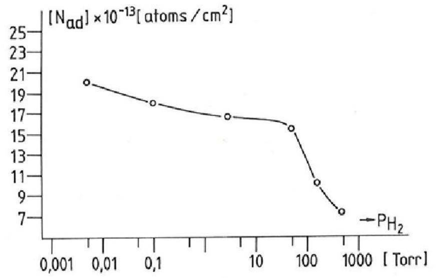

Figure 8.17 Variation of the surface concentration of atomic nitrogen ($[N_{ad}]$ in the diagram; N_a in the text), in arbitrary units, of a Fe (111) surface with the H_2 pressure after treatment in N_2/H_2 mixtures with a constant N_2 pressure of 150 Torr at 580 K. (After G. Ertl, *Catalysis*, **1983**, *4*, 210.)

The reaction proceeds through the atomic route and formation of $N_{(ad)}$ in the rate determining step.

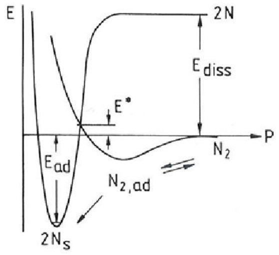

Figure 8.18 Potential-energy diagram for dissociative adsorption of nitrogen on iron. The activation energy E^* varies with surface structure as well as coverage. The adsorption energy E_{ad} is *ca* 200 kJ mol^{-1}. (After G. Ertl, *Angew. Chem. Int. Ed. Engl.*, **1990**, *29*, 1219.)

Ammonia synthesis

Reaction steps

$H_2 \rightleftharpoons 2\,H(ad)$

$N_2 \rightleftharpoons N_2(ad) \rightleftharpoons 2\,N(ad)$

$N(ad) + H(ad) \rightleftharpoons NH(ad)$

$NH_2(ad) + H(ad) \rightleftharpoons NH_2(ad)$

$NH_2(ad) + H(ad) \rightleftharpoons NH_3(ad)$

$NH_3(ad) \rightleftharpoons NH_3$

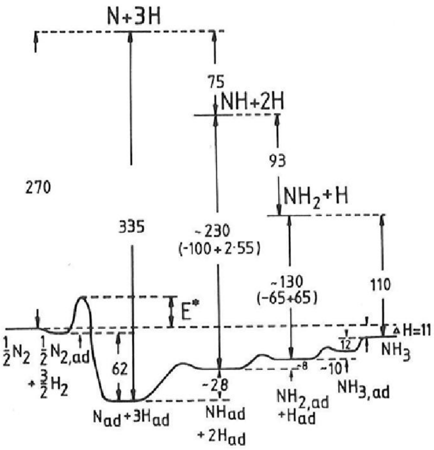

Potential energy diagram

Figure 8.21 Potential-energy diagram illustrating the progress of the catalytic synthesis of NH_3 on iron. (After G. Ertl, *Catalysis*, **1983**, *4*, 210.)

Ammonia synthesis

Effect of K

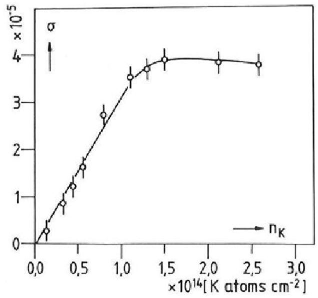

K increases the sticking coefficient for N_2.

Figure 8.23 Variation of the initial sticking coefficient for dissociative N_2 adsorption, σ, with concentration of potassium n_k on an Fe {100} surface at 430 K. (After G. Ertl, S. B. Lee, M. Weiss, *Surf. Sci.*, **1981**, *108*, 357.)

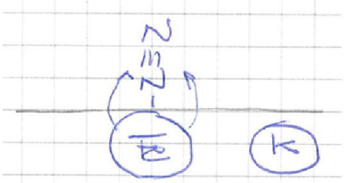

To favor N_2 dissociation, back-donation must be promoted.

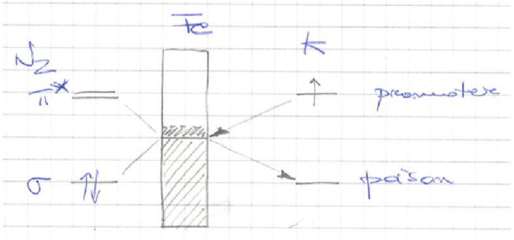

Air pollution

MOBILE SOURCES

EXHAUST

HYDROCARBONS (HC)

CARBON MONOXIDE (CO)

NITROGEN OXIDES (NO_X)

SULFUR COMPOUNDS

PM10

Possible solutions

Hydrogen car

Fuel cell

Electric car

Technical problem - batteries

Hybrid car

Catalytic converters – TWC

Cycling - walking

CH_4 & GREENHOUSE EFFECT

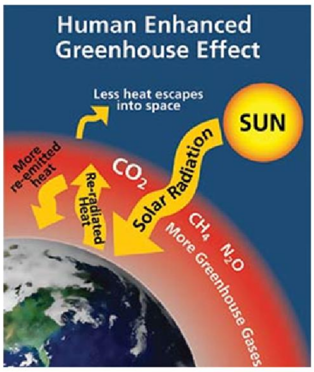

- Lifetime in the atmosphere is much shorter than CO_2
- More efficient at trapping radiation than CO_2

Impact of CH_4 on climate change is more than
25 times greater than CO_2

NEEDS FOR CATALYTIC ABATEMENT

Source Identification and Quantification

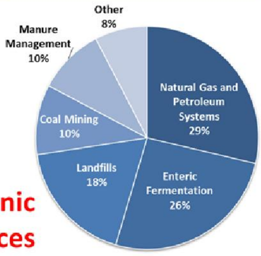

Anthropogenic sources

EPA, Emission Overvie

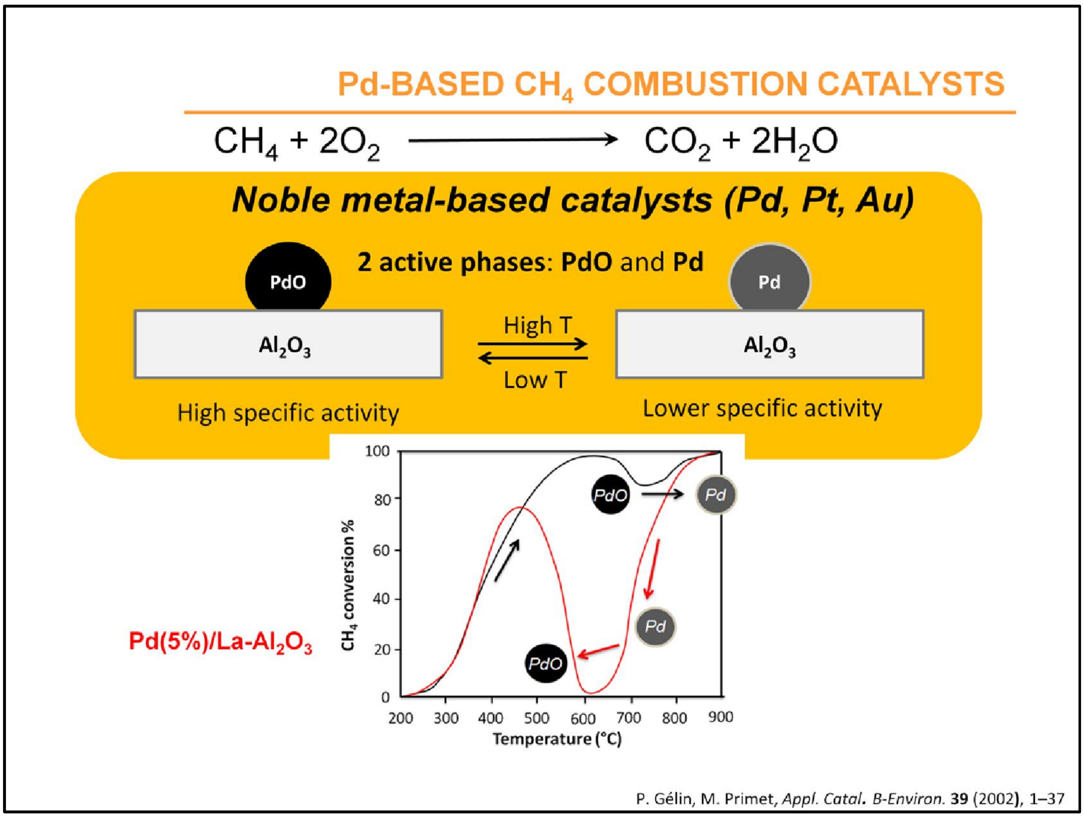

Pd-BASED CH_4 COMBUSTION CATALYSTS

$$CH_4 + 2O_2 \longrightarrow CO_2 + 2H_2O$$

Noble metal-based catalysts (Pd, Pt, Au)

2 active phases: **PdO** and **Pd**

PdO

Al_2O_3

High specific activity

$\xrightarrow{\text{High T}}$ / $\xleftarrow{\text{Low T}}$

Pd

Al_2O_3

Lower specific activity

Pd(5%)/La-Al_2O_3

P. Gélin, M. Primet, *Appl. Catal. B-Environ.* **39** (2002), 1–37

Pd-BASED CH_4 COMBUSTION CATALYSTS

Catalyze re-oxidation

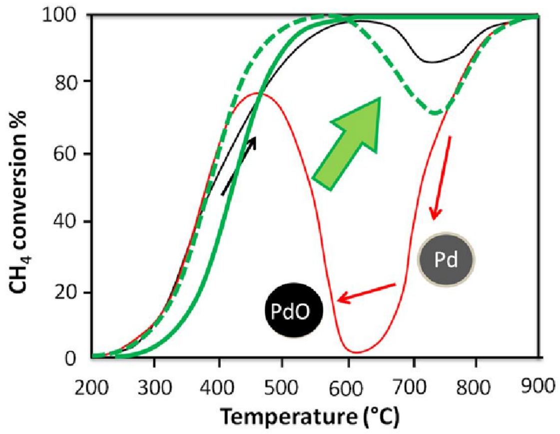

Maximize PdO - CeO_2 interaction

O_2 from the gas phase

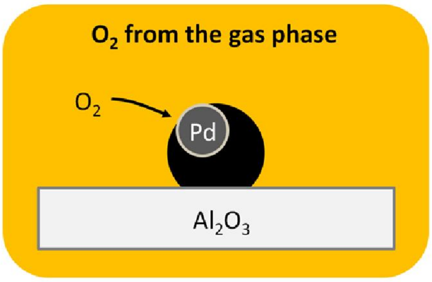

O_2 from a PROMOTER

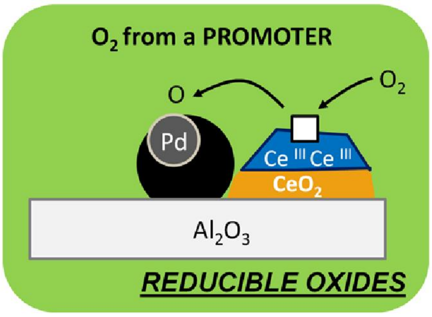

REDUCIBLE OXIDES

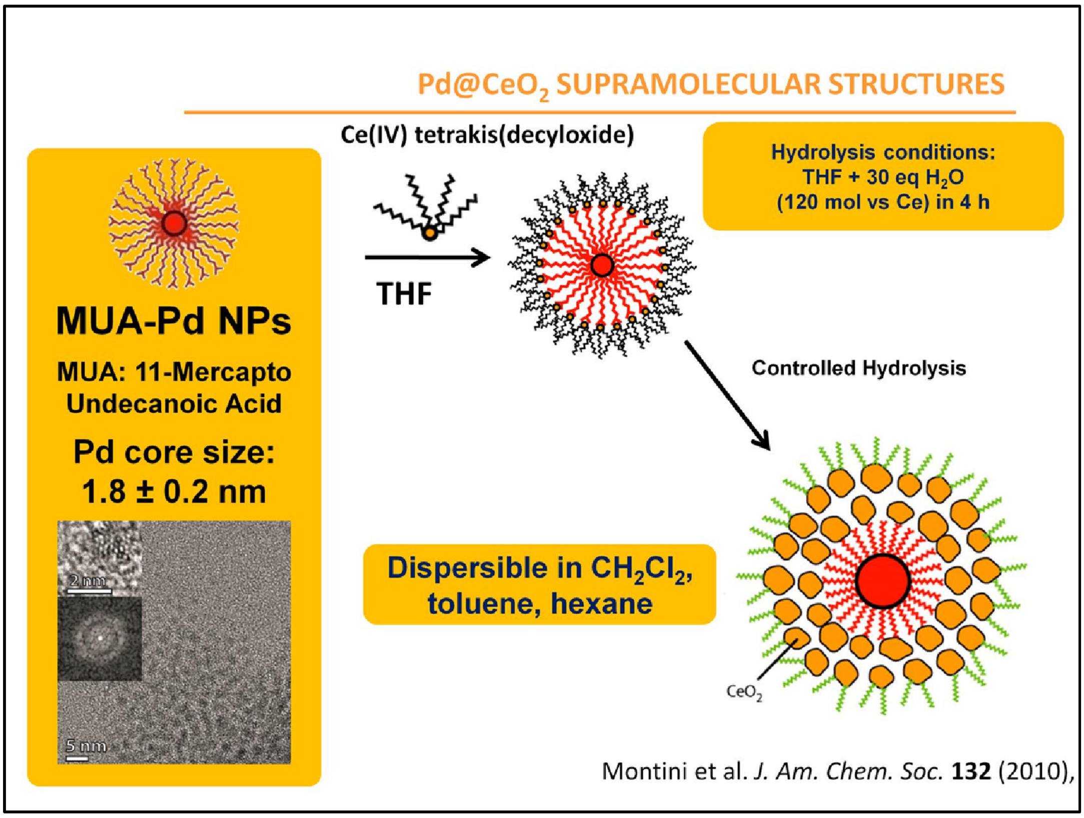

Pd@CeO$_2$ SUPRAMOLECULAR STRUCTURES

MUA-Pd NPs

MUA: 11-Mercapto Undecanoic Acid

Pd core size: 1.8 ± 0.2 nm

Hydrolysis conditions:
THF + 30 eq H_2O
(120 mol vs Ce) in 4 h

Dispersible in CH_2Cl_2, toluene, hexane

Montini et al. *J. Am. Chem. Soc.* **132** (2010),

Pd@CeO_2 FOR CH_4 COMBUSTION

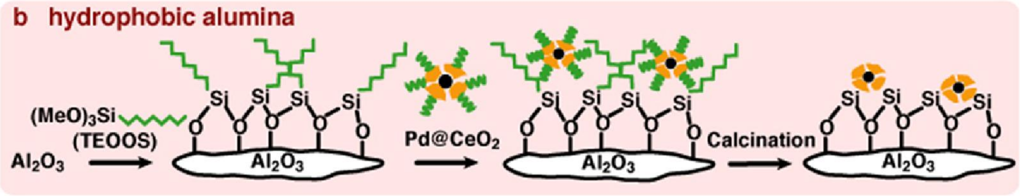

HAADF-STEM

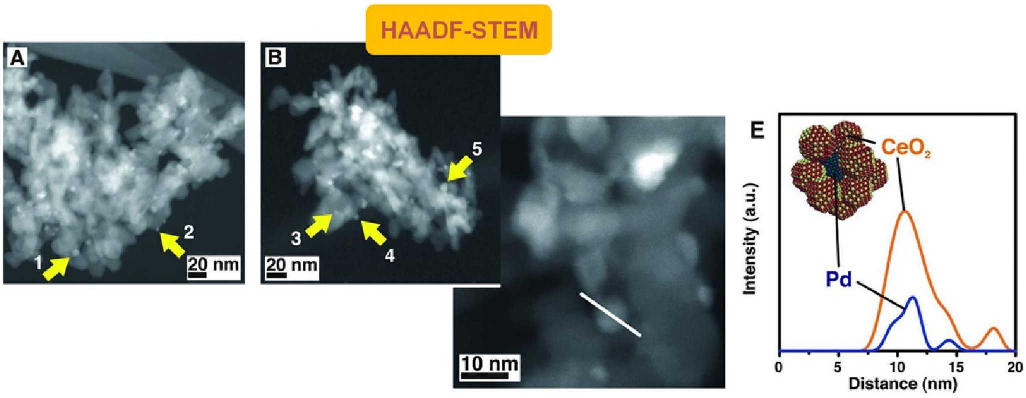

Montini et al. *Science* **337** (2012), 713-717.

Pd@CeO$_2$ FOR CH$_4$ COMBUSTION

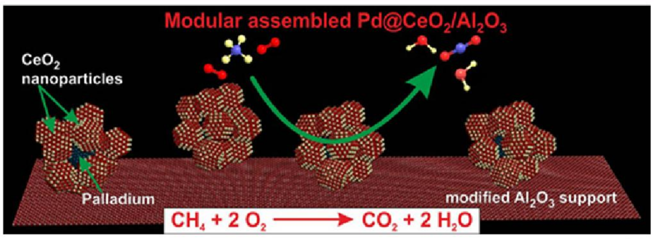

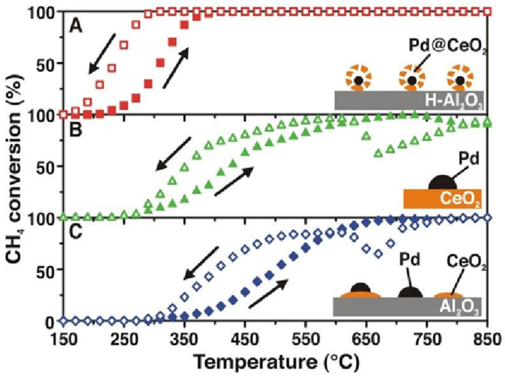

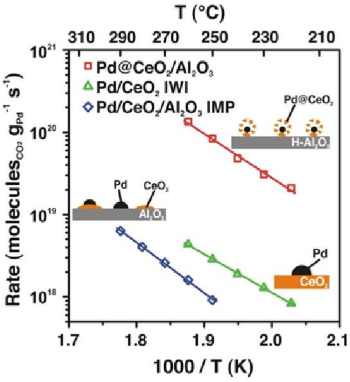

Montini et al. *Science* **337** (2012), 713-717.

Pd@CeO$_2$ FOR CH$_4$ COMBUSTION

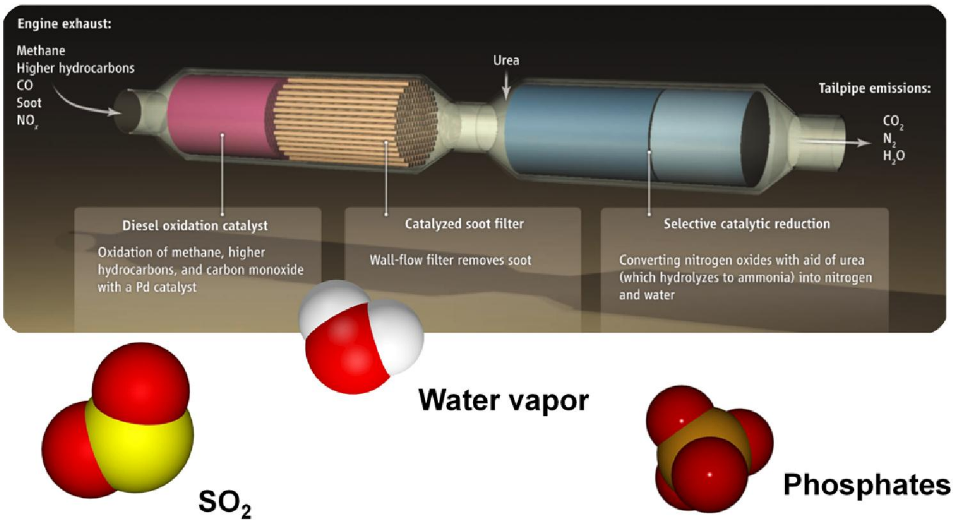

PdO DEACTIVATION

R. Farrauto, *Science* **337** (2012), 659

Pd@CeO$_2$ FOR CH$_4$ COMBUSTION

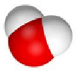

Light Off

Effect of water

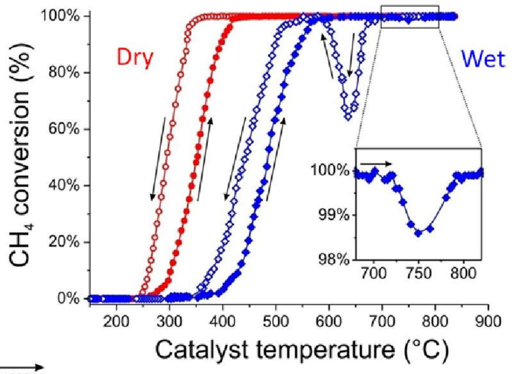

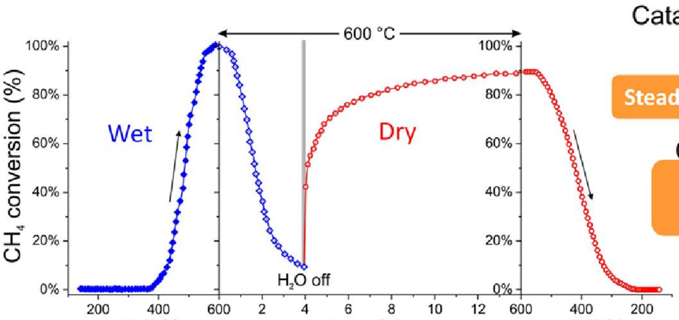

Steady State

0.5% CH_4, 2.0% O_2, 15% H_2O (if present), Ar balance, $O_2/O_{2(stoich)}$=2, GHSV = 200000 mL g^{-1} h^{-1}

Montini et al. *ChemCatChem* **7** (2015), 2038-

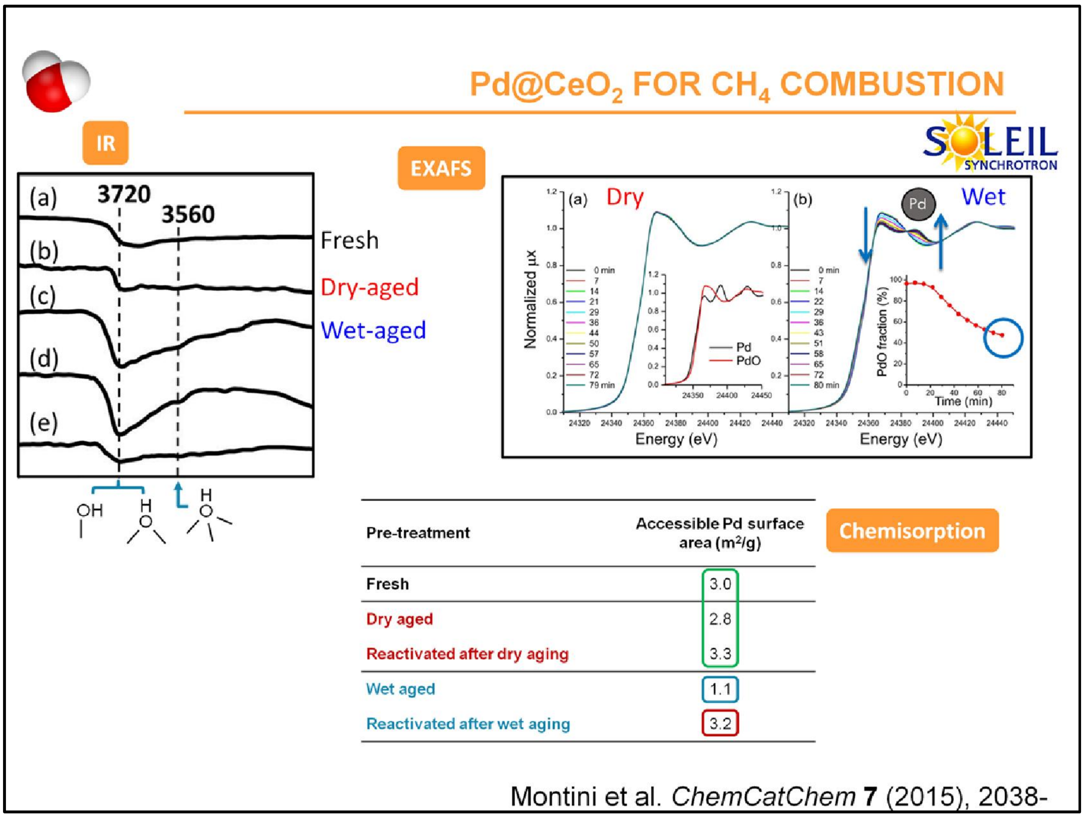

Pd@CeO$_2$ FOR CH$_4$ COMBUSTION

Pre-treatment	Accessible Pd surface area (m^2/g)
Fresh	3.0
Dry aged	2.8
Reactivated after dry aging	3.3
Wet aged	1.1
Reactivated after wet aging	3.2

Montini et al. *ChemCatChem* **7** (2015), 2038-

Pd@CeO$_2$ FOR CH$_4$ COMBUSTION

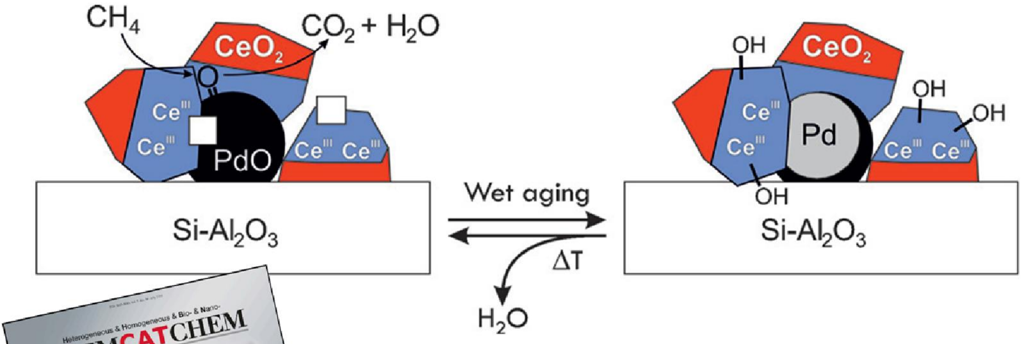

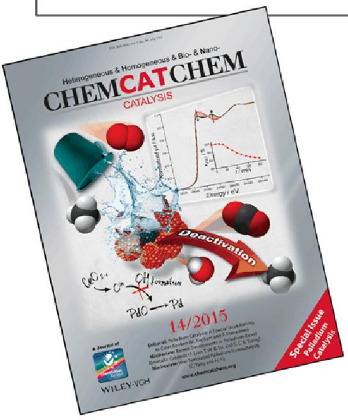

- **Reduction of PdO to Pd**
- **Increase in population of OH**
- **Wet aging reduces Pd accessibility**

Montini et al. *ChemCatChem* **7** (2015), 2038-

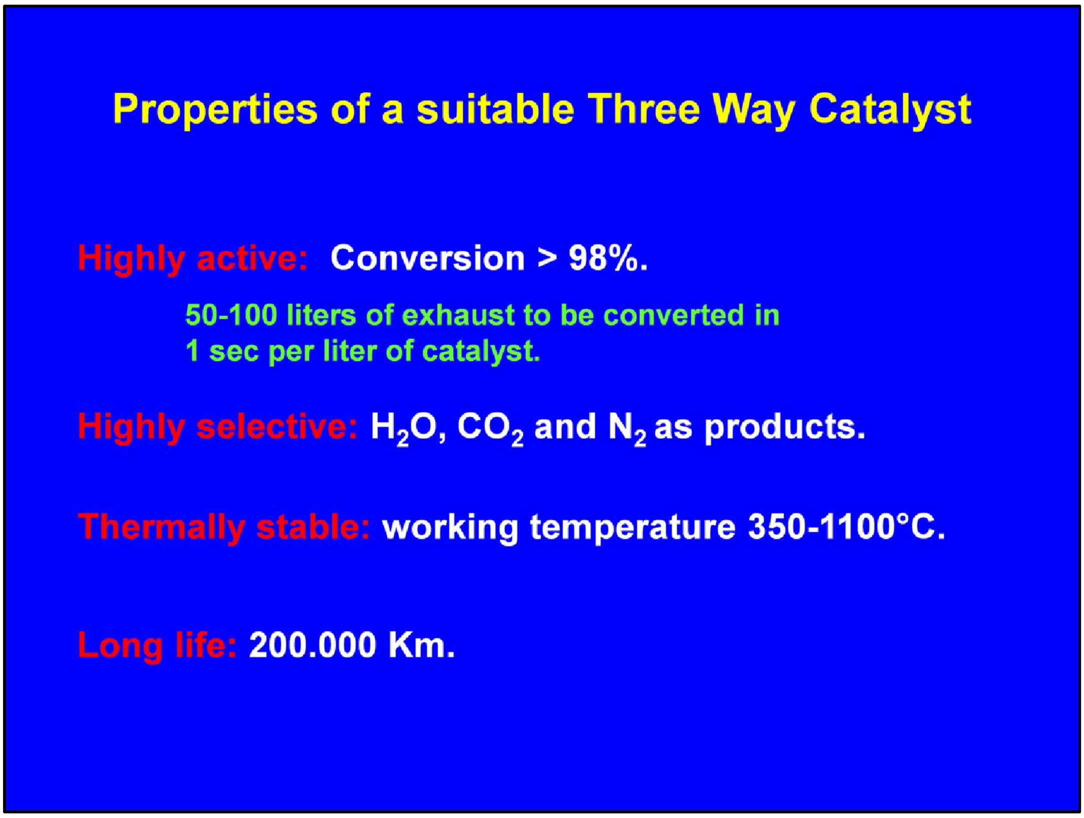

Properties of a suitable Three Way Catalyst

Highly active: Conversion > 98%.

50-100 liters of exhaust to be converted in
1 sec per liter of catalyst.

Highly selective: H_2O, CO_2 and N_2 as products.

Thermally stable: working temperature 350-1100°C.

Long life: 200.000 Km.

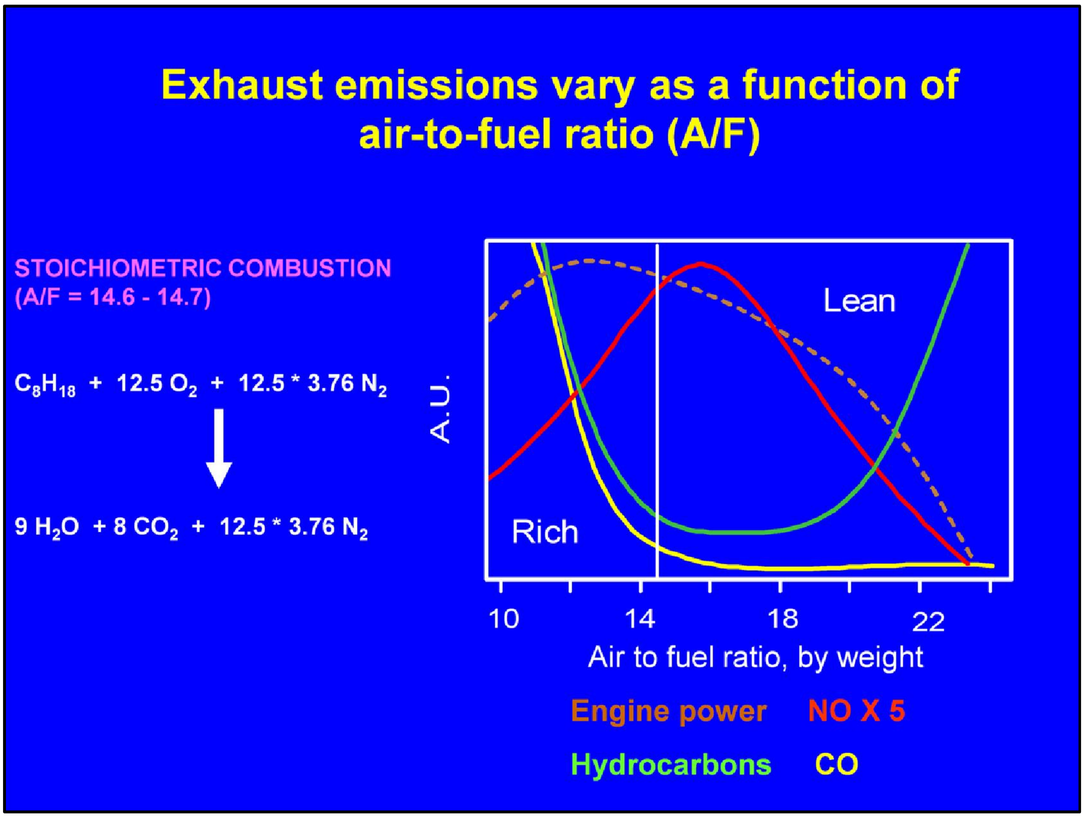

Exhaust emissions vary as a function of air-to-fuel ratio (A/F)

STOICHIOMETRIC COMBUSTION
(A/F = 14.6 - 14.7)

$$C_8H_{18} + 12.5\ O_2 + 12.5 * 3.76\ N_2$$

$$\downarrow$$

$$9\ H_2O + 8\ CO_2 + 12.5 * 3.76\ N_2$$

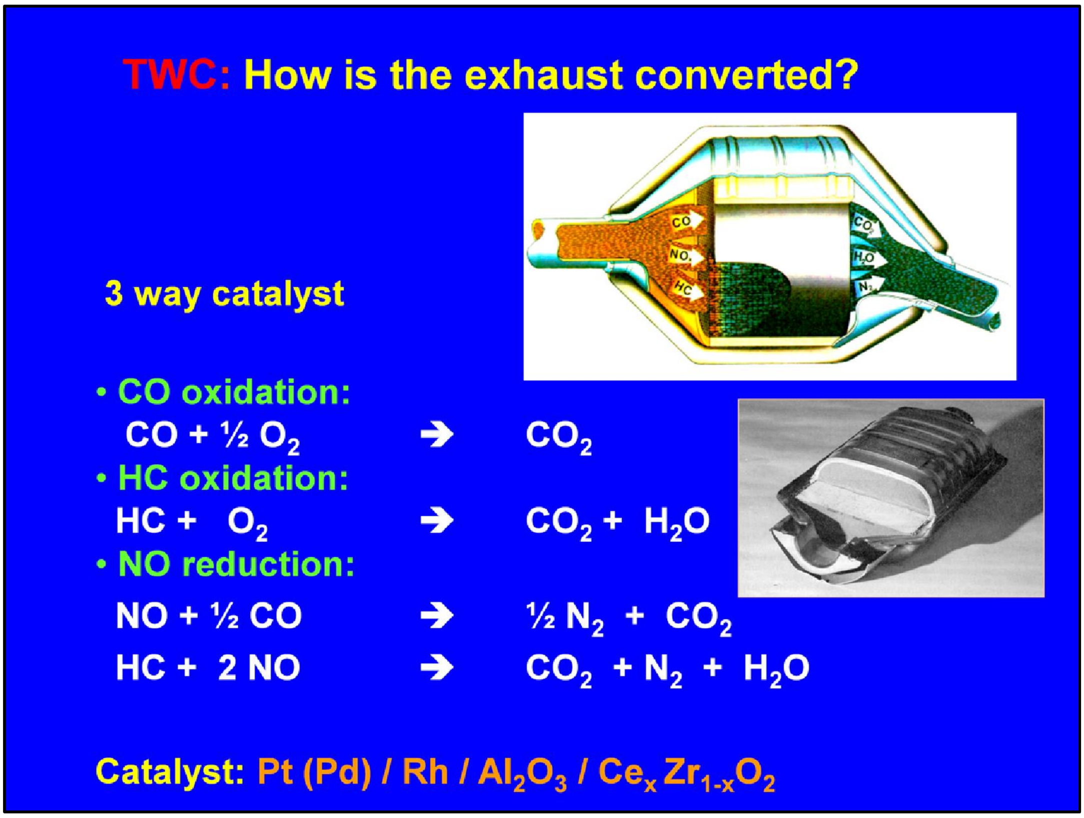

TWC: How is the exhaust converted?

3 way catalyst

- **CO oxidation:**
  $CO + \frac{1}{2} O_2 \rightarrow CO_2$
- **HC oxidation:**
  $HC + O_2 \rightarrow CO_2 + H_2O$
- **NO reduction:**
  $NO + \frac{1}{2} CO \rightarrow \frac{1}{2} N_2 + CO_2$
  $HC + 2\,NO \rightarrow CO_2 + N_2 + H_2O$

Catalyst: Pt (Pd) / Rh / Al_2O_3 / $Ce_x Zr_{1-x}O_2$

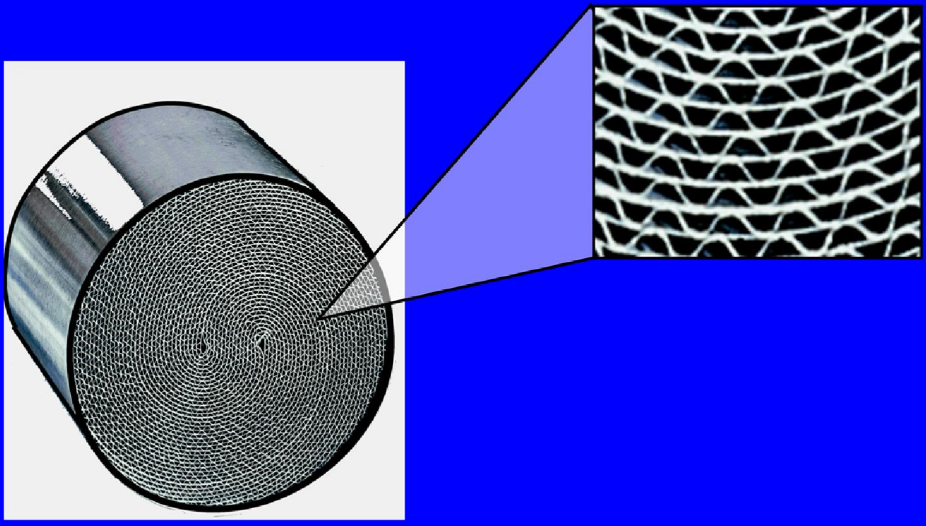

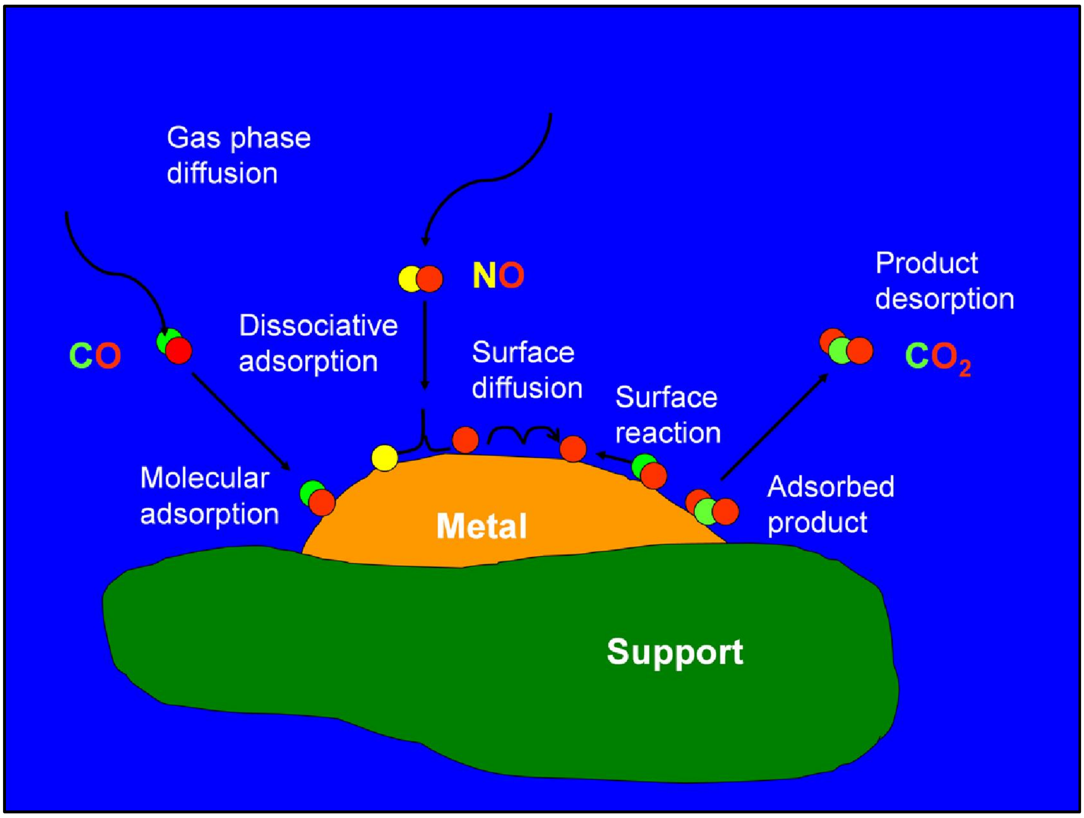
Gas phase diffusion
NO
Product desorption
CO
Dissociative adsorption
Surface diffusion
CO_2
Surface reaction
Molecular adsorption
Adsorbed product
Metal
Support

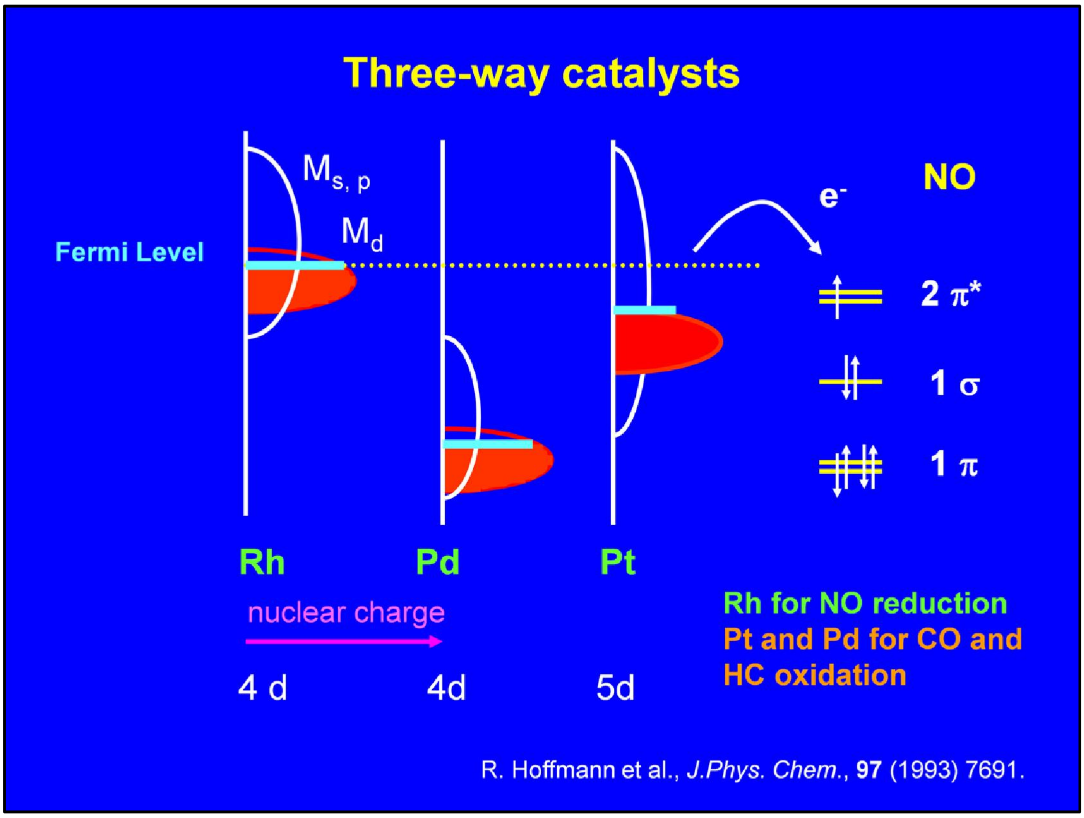

Three-way catalysts

Rh for NO reduction

Pt and Pd for CO and HC oxidation

R. Hoffmann et al., *J.Phys. Chem.*, **97** (1993) 7691.

Temperature dependence of conversions

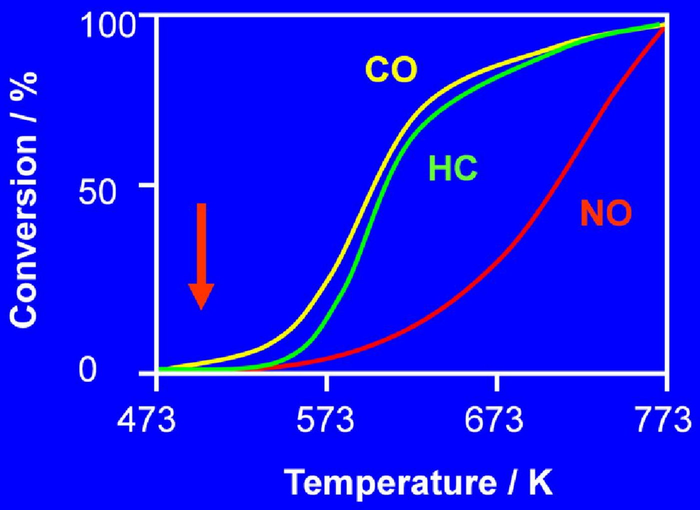

Three-way catalyst

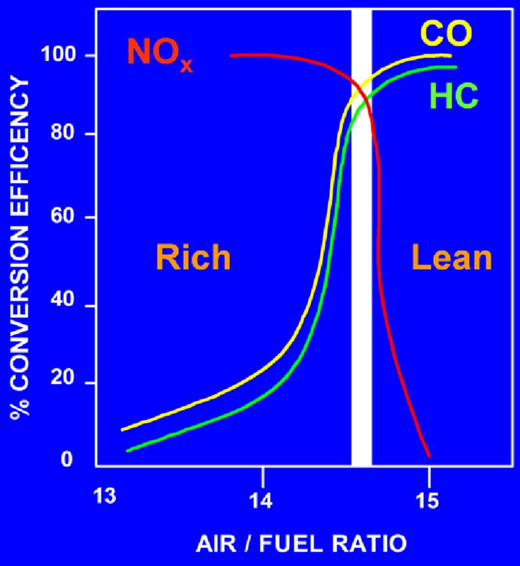

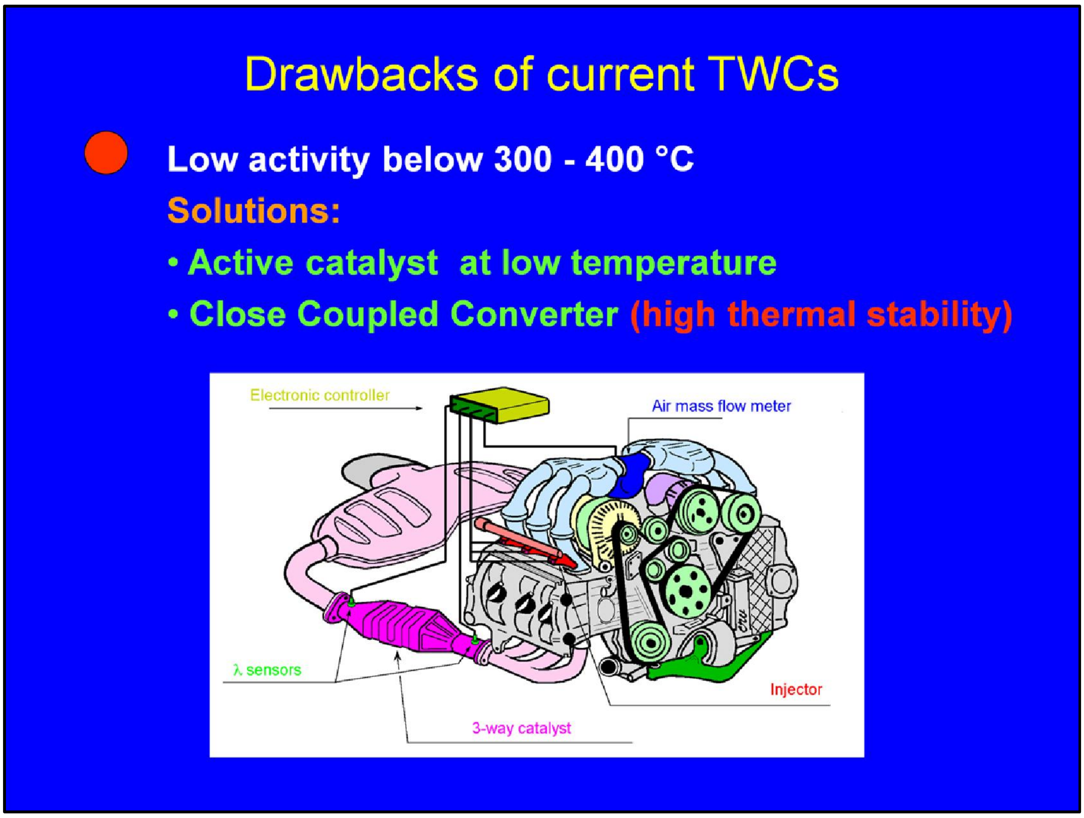

Drawbacks of current TWCs

- **Low activity below 300 - 400 °C**

Solutions:

- **Active catalyst at low temperature**
- **Close Coupled Converter (high thermal stability)**

Oxygen buffer in TWCs

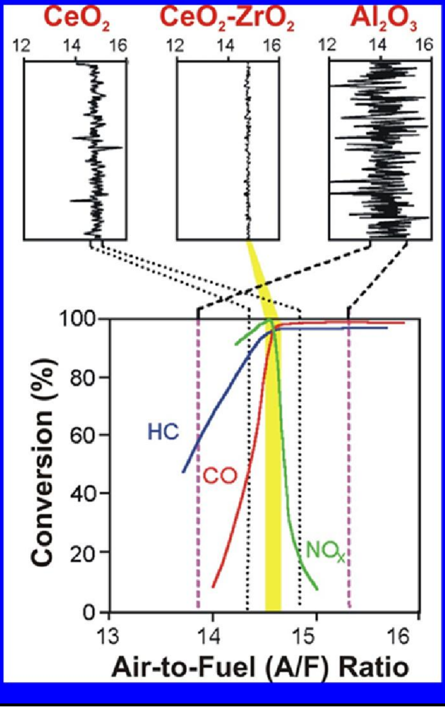

Need A/F close to the stoichiometric value

$$2CeO_2 \Leftrightarrow CeO_{2-x} + x/2\ O_2$$

CeO_2 is an oxygen buffer

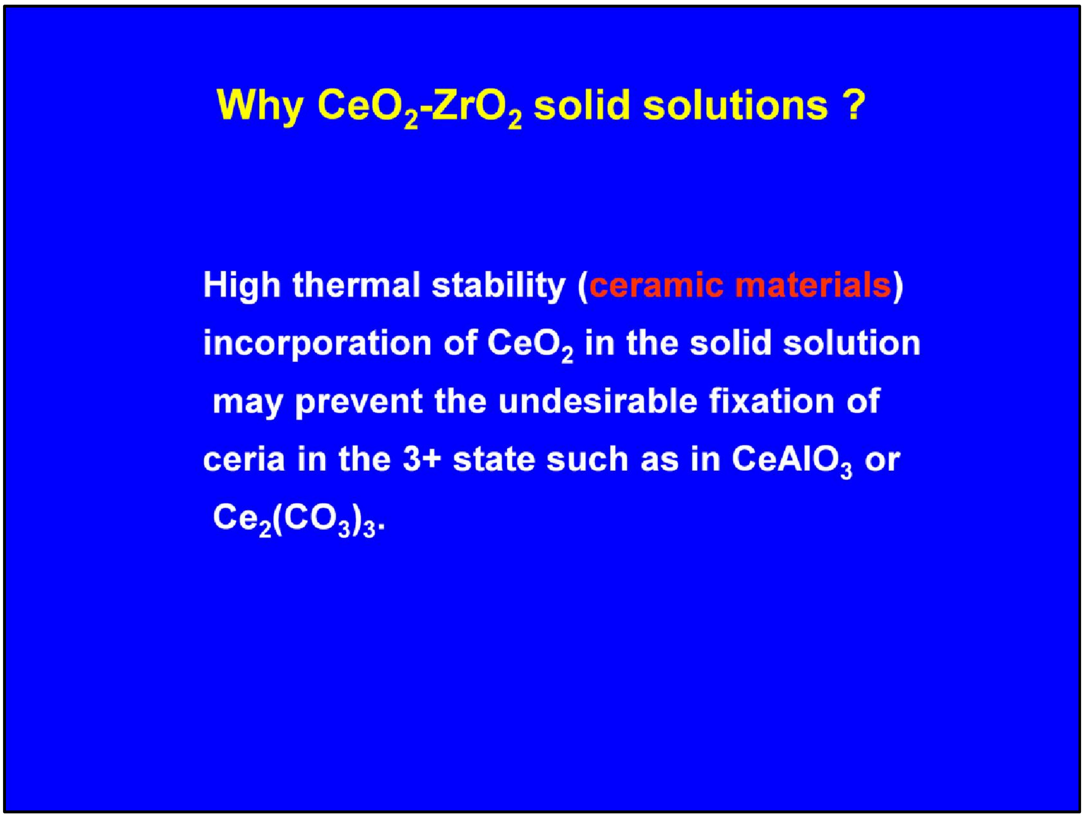

Why CeO_2-ZrO_2 solid solutions ?

High thermal stability (ceramic materials) incorporation of CeO_2 in the solid solution may prevent the undesirable fixation of ceria in the 3+ state such as in $CeAlO_3$ or $Ce_2(CO_3)_3$.

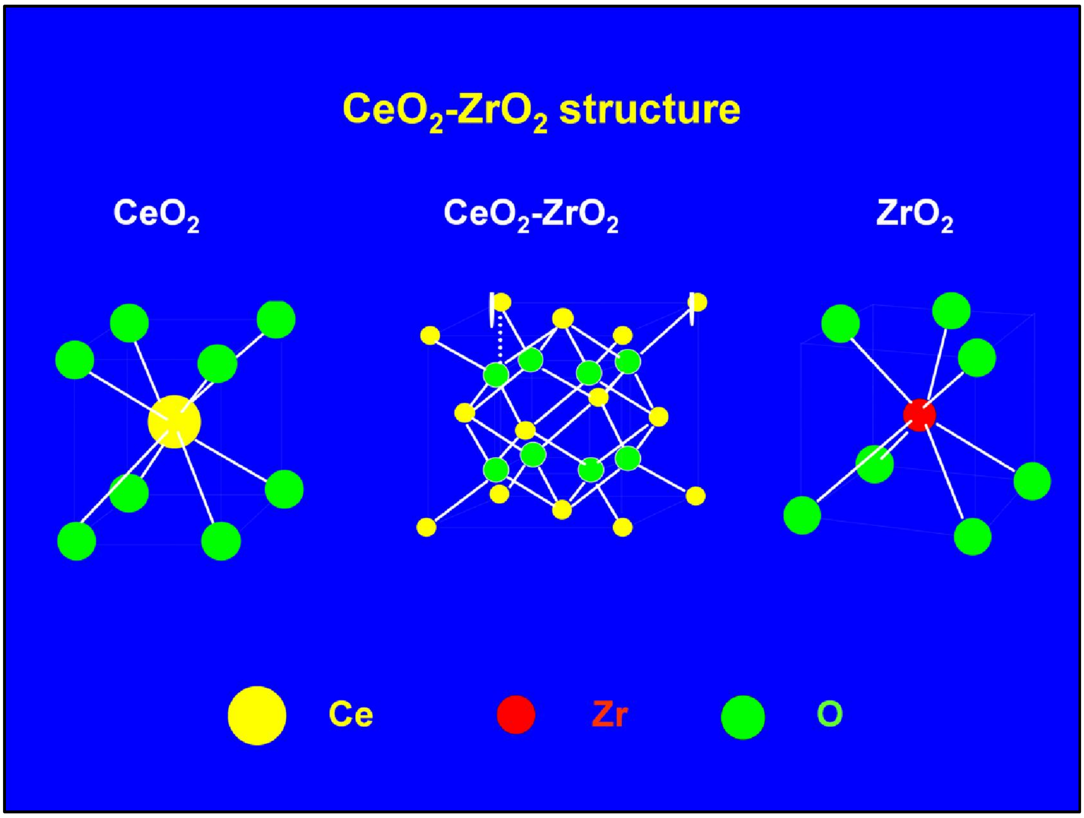

CeO_2-ZrO_2 structure

CeO_2 CeO_2-ZrO_2 ZrO_2

● Ce ● Zr ● O

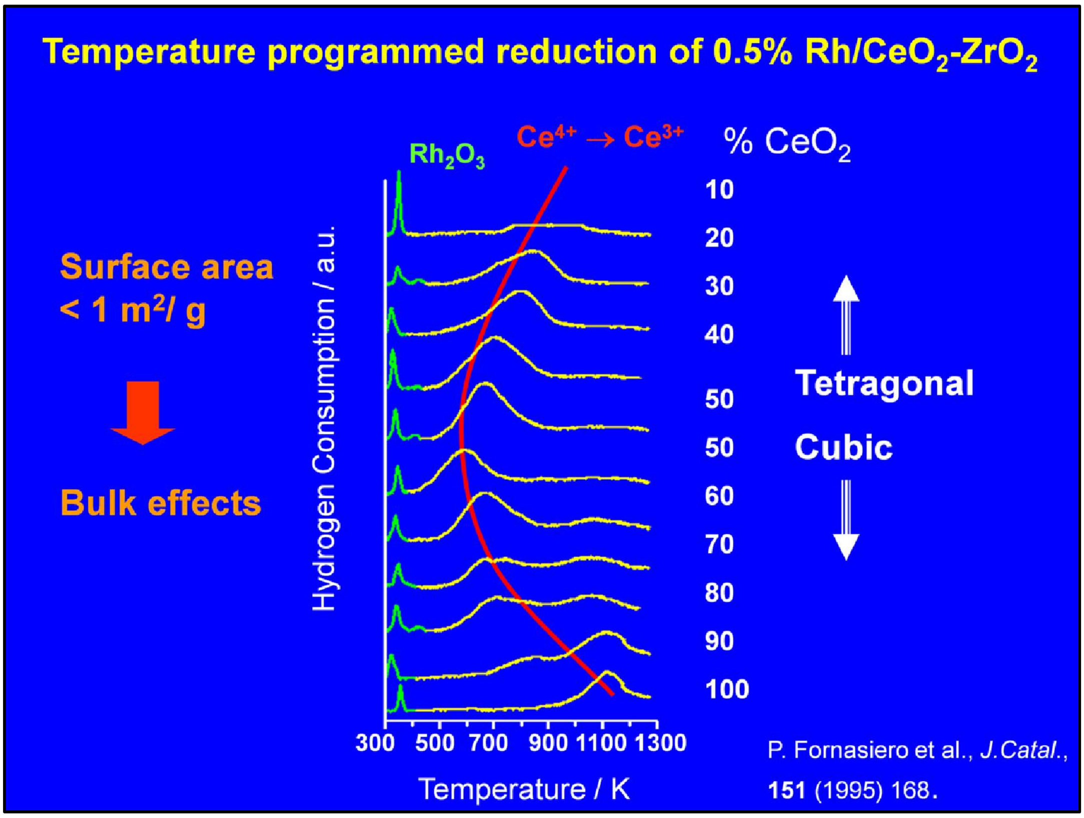

Temperature programmed reduction of 0.5% Rh/CeO_2-ZrO_2

Surface area < 1 m^2/ g

Bulk effects

P. Fornasiero et al., *J.Catal.*, **151** (1995) 168.

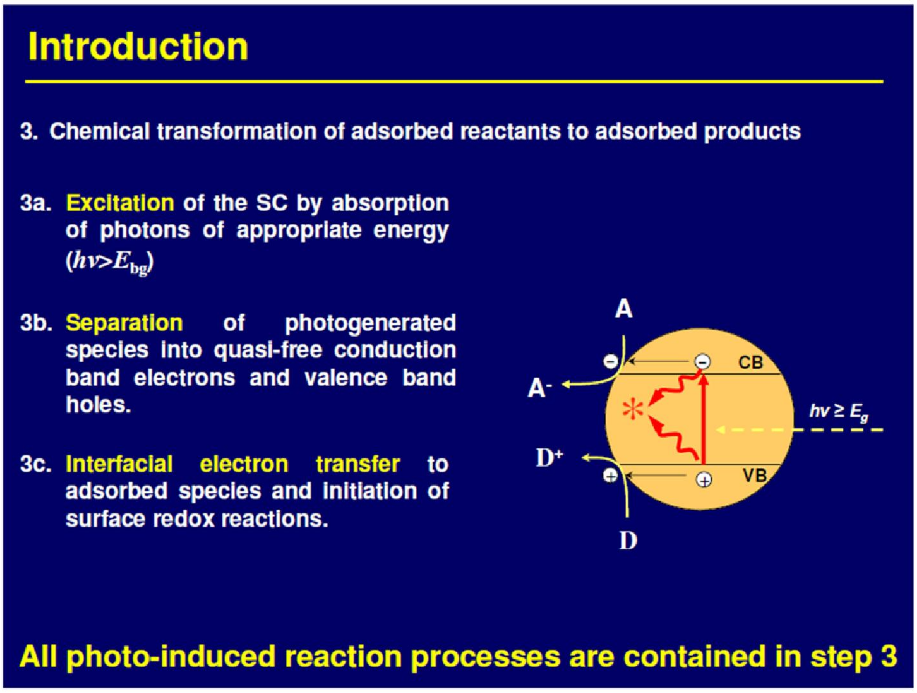

Introduction

3. Chemical transformation of adsorbed reactants to adsorbed products

3a. **Excitation** of the SC by absorption of photons of appropriate energy ($h\nu > E_{bg}$)

3b. **Separation** of photogenerated species into quasi-free conduction band electrons and valence band holes.

3c. **Interfacial electron transfer** to adsorbed species and initiation of surface redox reactions.

All photo-induced reaction processes are contained in step 3

Generation and fate of charge carriers

Excitation: $\mathrm{SC} + h\nu \rightarrow e^-_{\mathrm{CB}} + h^+_{\mathrm{VB}}$

Recombination: $e^-_{\mathrm{CB}} + h^+_{\mathrm{VB}} \rightarrow \text{energy}$

Trapping: $e^-_{\mathrm{CB}} \rightarrow e^-_{\mathrm{tr}}$

$h^+_{\mathrm{VB}} \rightarrow h^+_{\mathrm{tr}}$

In the presence of an electric field of sufficient intensity to overcome Coulombic attraction forces, the exciton may be separated in quasi free electrons (CB) and holes (VB)

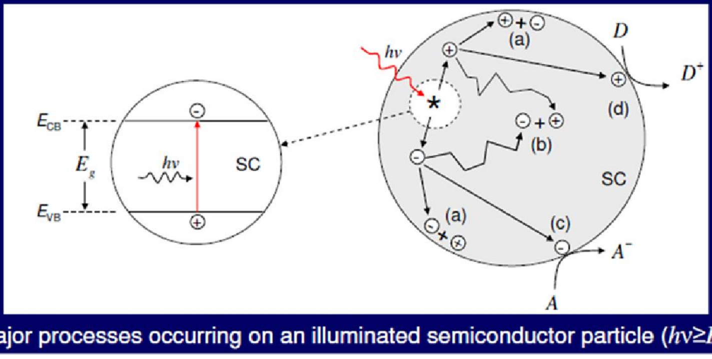

Major processes occurring on an illuminated semiconductor particle ($h\nu \geq E_g$)

Interfacial charge transfer and redox reactions

Interfacial charge transfer:

$$A_{(ad)} + e^-_{tr} \rightarrow A^{-\bullet}_{(ad)}$$

$$D_{(ad)} + h^+_{tr} \rightarrow D^{+\bullet}_{(ad)}$$

Dark reactions must be much faster than recombination reactions.

Redox reactions:

$$A^{-\bullet}_{(ad)} \rightarrow \ldots \rightarrow B$$

$$D^{+\bullet}_{(ad)} \rightarrow \ldots \rightarrow C$$

$$e^-_{tr} + h^+_{tr} \rightarrow \text{energy}$$

$$A^{-\bullet}_{(ad)} + D^{+\bullet}_{(ad)} \rightarrow A_{(ad)} + D_{(ad)}$$

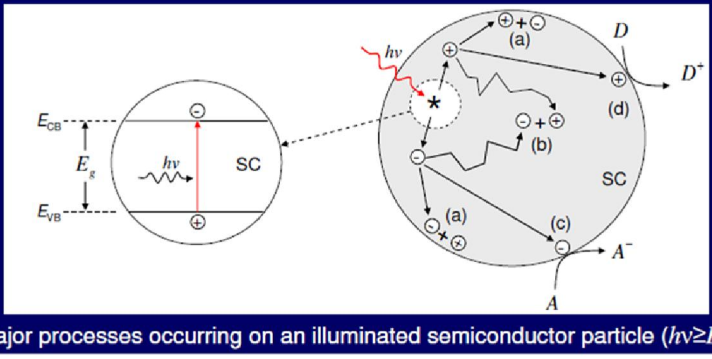

Major processes occurring on an illuminated semiconductor particle ($h\nu \geq E_g$)

Interfacial charge transfer and redox reactions

The ability of a photogenerated electron (or hole) to initiate a specific redox reaction depends on the relative position of E_{CB} (or E_{VB}) with respect to the redox potential of the adsorbed species.

For reduction of species A, E_{CB} has to be positioned above the energy level of A/A^- couple.

For oxidation of species D, E_{VB} has to be positioned below the energy level of the D/D^+ couple.

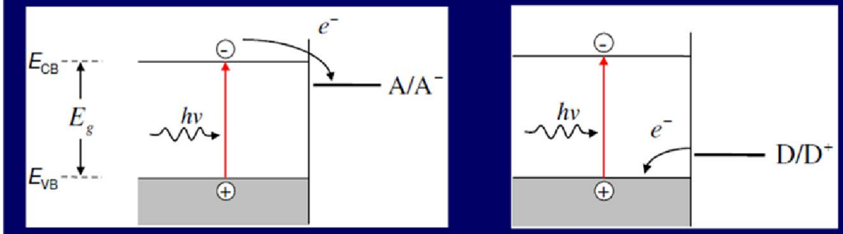

Interfacial charge transfer by capture of (a) a photogenerated electron by an electron acceptor and (b) a photogenerated hole by an electron donor.

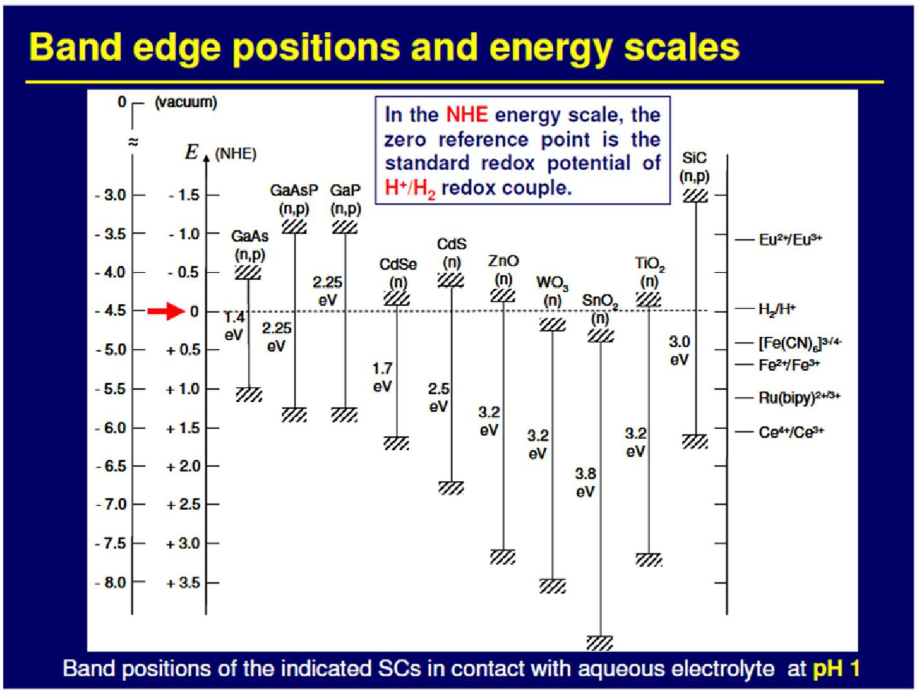

Band edge positions and energy scales

In the **NHE** energy scale, the zero reference point is the standard redox potential of **H^+/H_2** redox couple.

Band positions of the indicated SCs in contact with aqueous electrolyte at **pH 1**

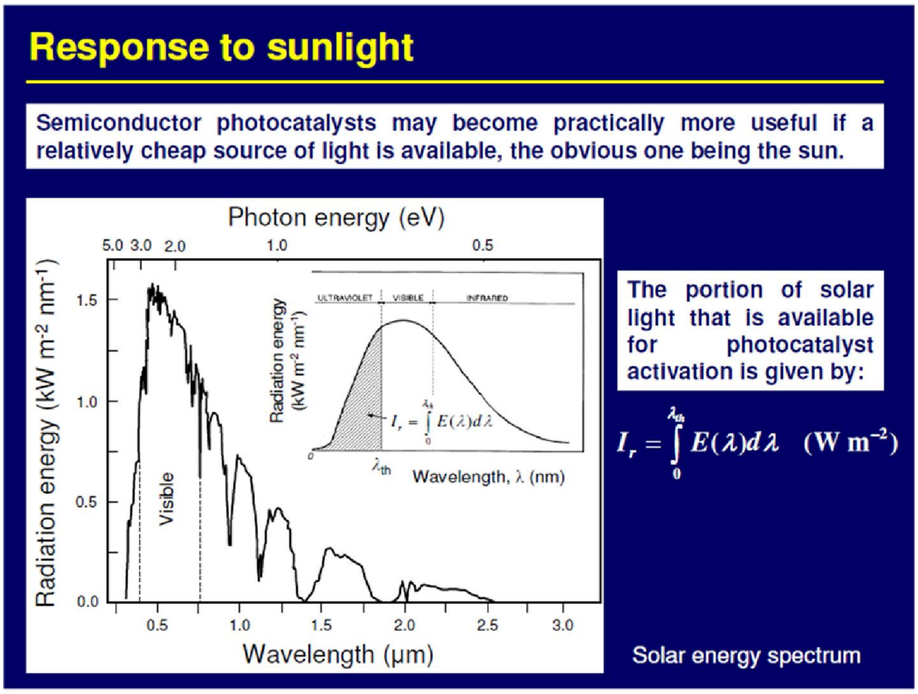

Response to sunlight

Semiconductor photocatalysts may become practically more useful if a relatively cheap source of light is available, the obvious one being the sun.

$I_r = \int_0^{\lambda_{th}} E(\lambda)d\lambda$

The portion of solar light that is available for photocatalyst activation is given by:

$$I_r = \int_0^{\lambda_{th}} E(\lambda)d\lambda \quad (\mathrm{W\ m^{-2}})$$

Solar energy spectrum

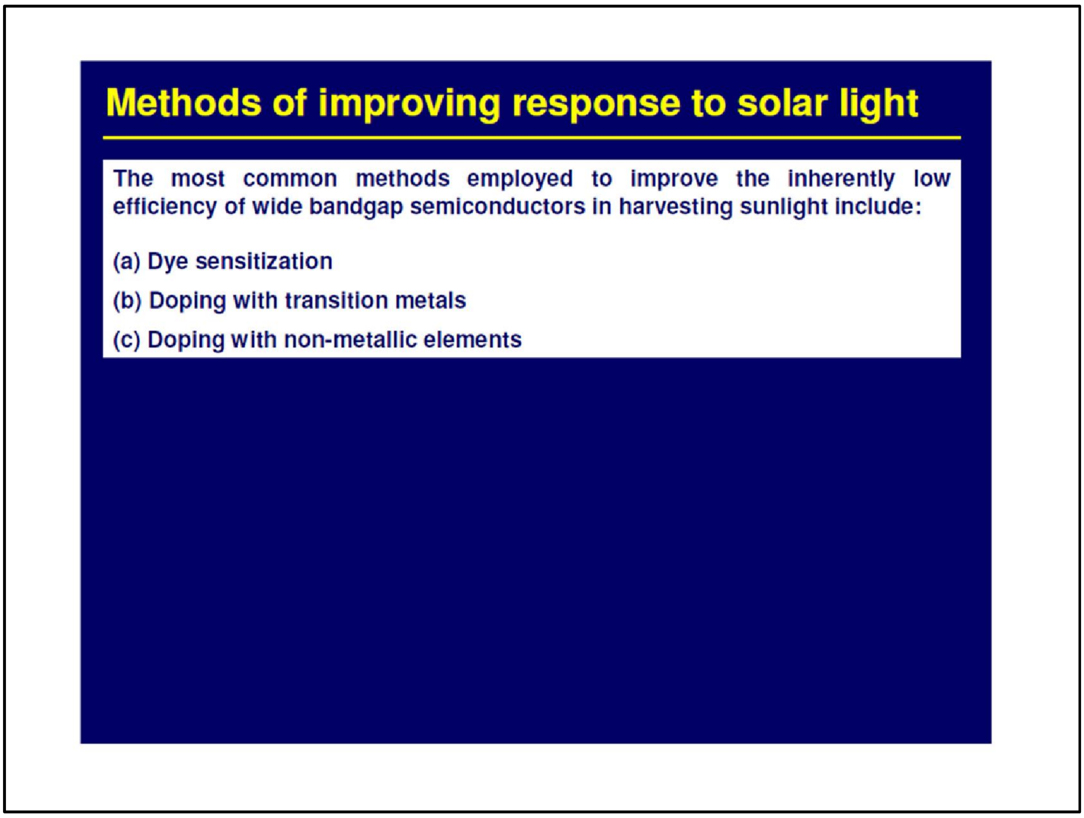

Methods of improving response to solar light

The most common methods employed to improve the inherently low efficiency of wide bandgap semiconductors in harvesting sunlight include:

(a) Dye sensitization

(b) Doping with transition metals

(c) Doping with non-metallic elements

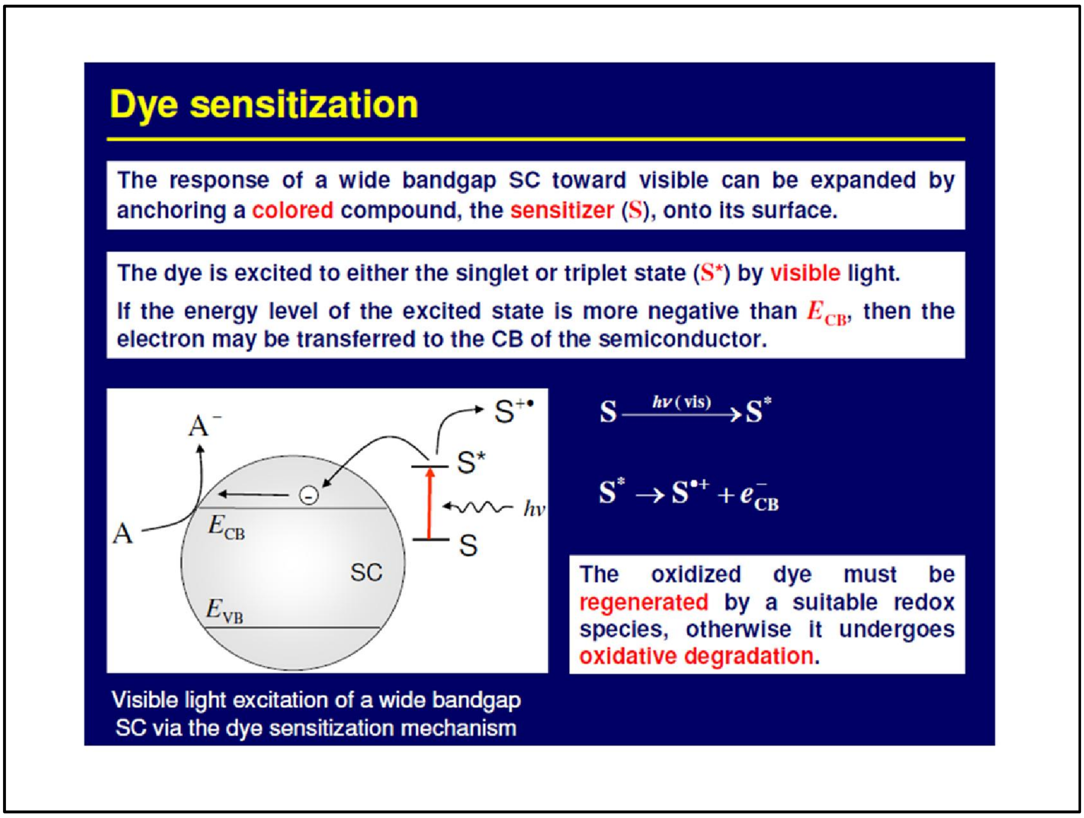

Dye sensitization

The response of a wide bandgap SC toward visible can be expanded by anchoring a colored compound, the sensitizer (S), onto its surface.

The dye is excited to either the singlet or triplet state (S*) by visible light.

If the energy level of the excited state is more negative than E_{CB}, then the electron may be transferred to the CB of the semiconductor.

$$S \xrightarrow{h\nu(\text{vis})} S^*$$

$$S^* \rightarrow S^{\bullet+} + e^-_{CB}$$

The oxidized dye must be regenerated by a suitable redox species, otherwise it undergoes oxidative degradation.

Visible light excitation of a wide bandgap SC via the dye sensitization mechanism

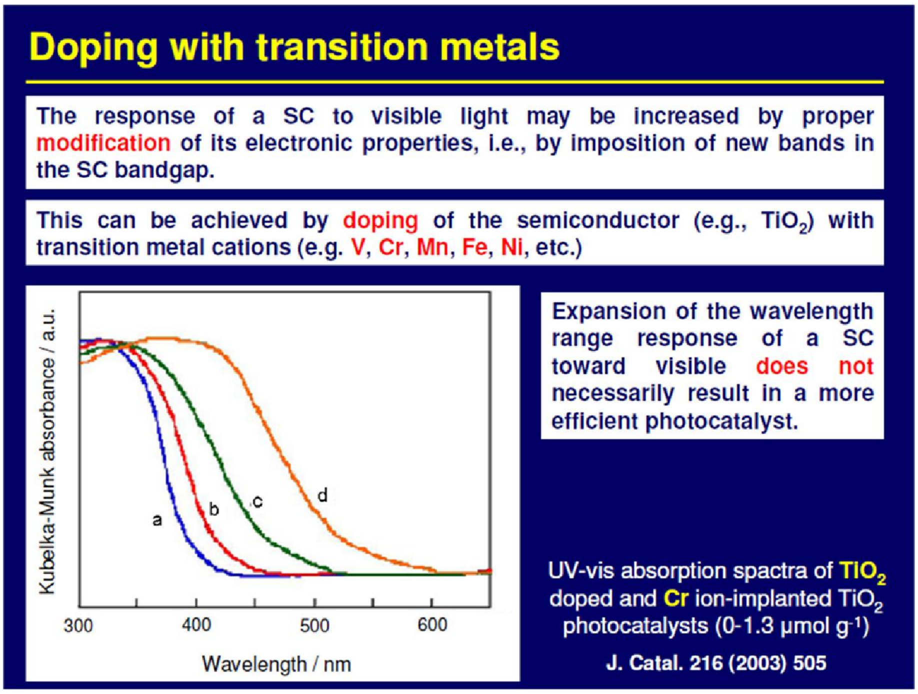

Doping with transition metals

The response of a SC to visible light may be increased by proper modification of its electronic properties, i.e., by imposition of new bands in the SC bandgap.

This can be achieved by doping of the semiconductor (e.g., TiO_2) with transition metal cations (e.g. V, Cr, Mn, Fe, Ni, etc.)

Expansion of the wavelength range response of a SC toward visible does not necessarily result in a more efficient photocatalyst.

UV-vis absorption spactra of TiO_2 doped and Cr ion-implanted TiO_2 photocatalysts (0-1.3 µmol g^{-1})

J. Catal. 216 (2003) 505

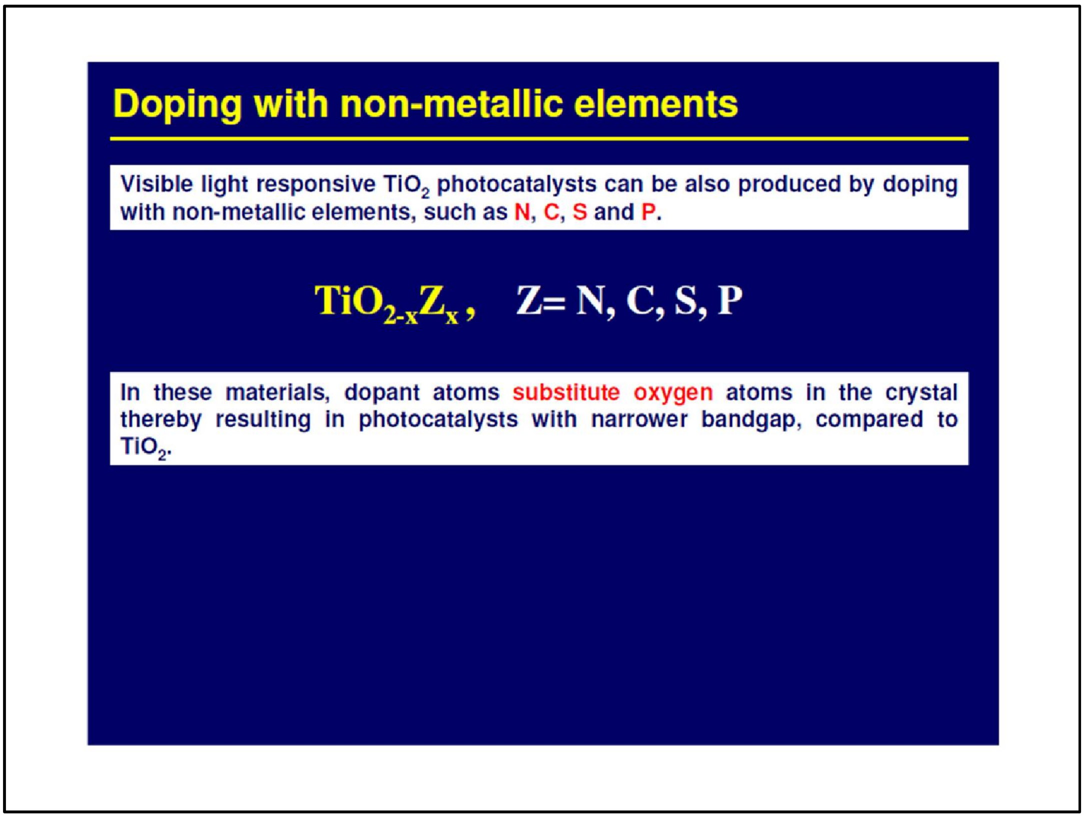

Doping with non-metallic elements

Visible light responsive TiO_2 photocatalysts can be also produced by doping with non-metallic elements, such as N, C, S and P.

$$TiO_{2-x}Z_x, \quad Z = N, C, S, P$$

In these materials, dopant atoms substitute oxygen atoms in the crystal thereby resulting in photocatalysts with narrower bandgap, compared to TiO_2.

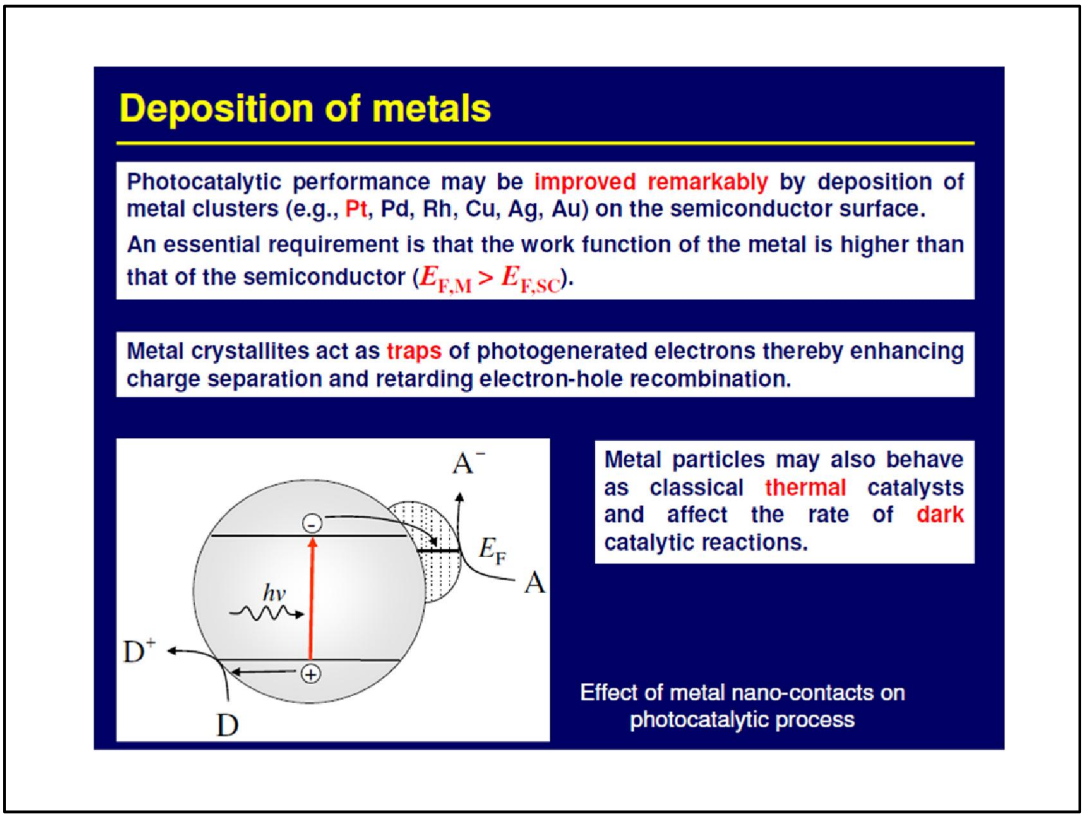

Deposition of metals

Photocatalytic performance may be improved remarkably by deposition of metal clusters (e.g., Pt, Pd, Rh, Cu, Ag, Au) on the semiconductor surface.

An essential requirement is that the work function of the metal is higher than that of the semiconductor ($E_{F,M} > E_{F,SC}$).

Metal crystallites act as traps of photogenerated electrons thereby enhancing charge separation and retarding electron-hole recombination.

Metal particles may also behave as classical thermal catalysts and affect the rate of dark catalytic reactions.

Effect of metal nano-contacts on photocatalytic process

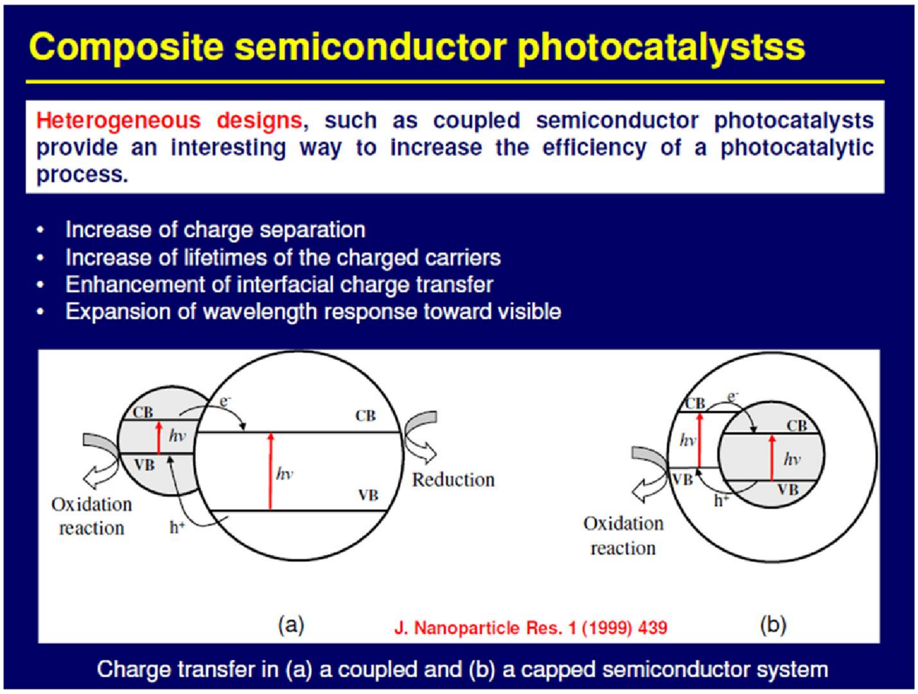

Composite semiconductor photocatalystss

Heterogeneous designs, **such as coupled semiconductor photocatalysts provide an interesting way to increase the efficiency of a photocatalytic process.**

- Increase of charge separation
- Increase of lifetimes of the charged carriers
- Enhancement of interfacial charge transfer
- Expansion of wavelength response toward visible

J. Nanoparticle Res. 1 (1999) 439

Charge transfer in (a) a coupled and (b) a capped semiconductor system

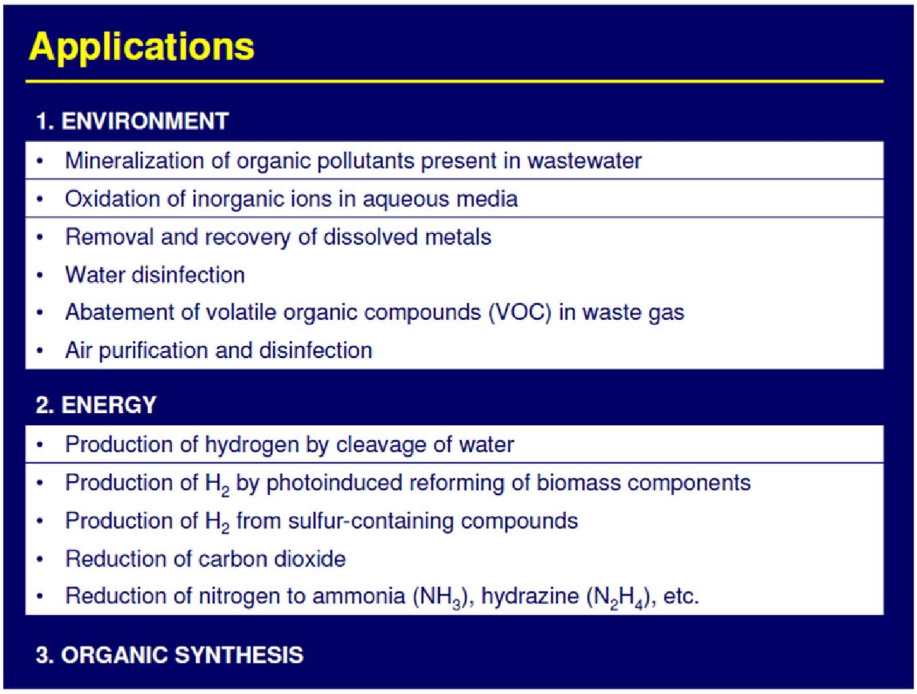

Applications

1. ENVIRONMENT

- Mineralization of organic pollutants present in wastewater
- Oxidation of inorganic ions in aqueous media
- Removal and recovery of dissolved metals
- Water disinfection
- Abatement of volatile organic compounds (VOC) in waste gas
- Air purification and disinfection

2. ENERGY

- Production of hydrogen by cleavage of water
- Production of H_2 by photoinduced reforming of biomass components
- Production of H_2 from sulfur-containing compounds
- Reduction of carbon dioxide
- Reduction of nitrogen to ammonia (NH_3), hydrazine (N_2H_4), etc.

3. ORGANIC SYNTHESIS

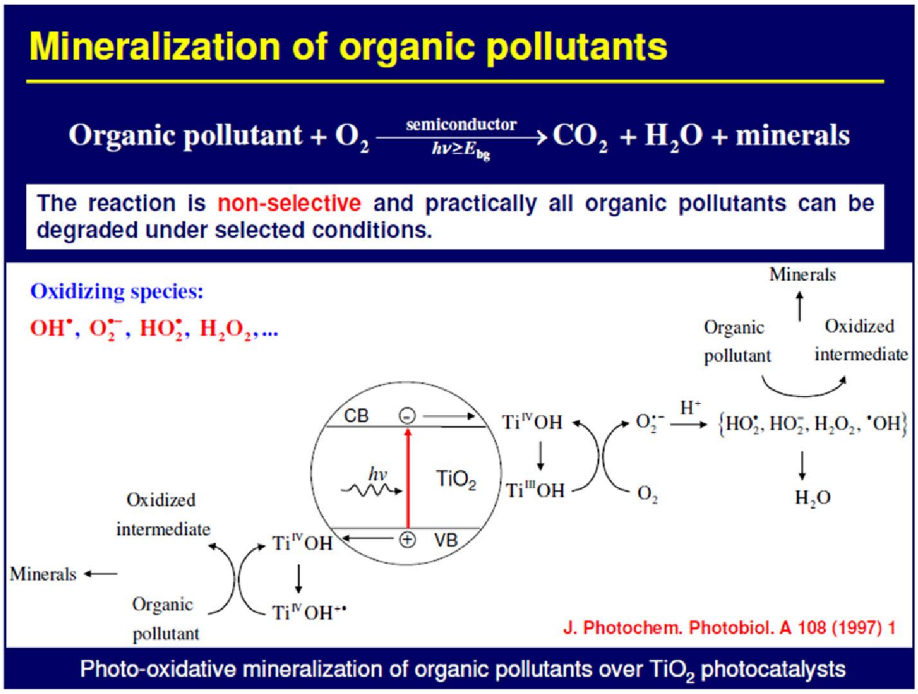

Mineralization of organic pollutants

$$\text{Organic pollutant} + O_2 \xrightarrow[h\nu \geq E_{bg}]{\text{semiconductor}} CO_2 + H_2O + \text{minerals}$$

The reaction is non-selective and practically all organic pollutants can be degraded under selected conditions.

Oxidizing species:

$OH^\bullet$, $O_2^{\bullet -}$, $HO_2^\bullet$, H_2O_2, ...

J. Photochem. Photobiol. A 108 (1997) 1

Photo-oxidative mineralization of organic pollutants over TiO_2 photocatalysts

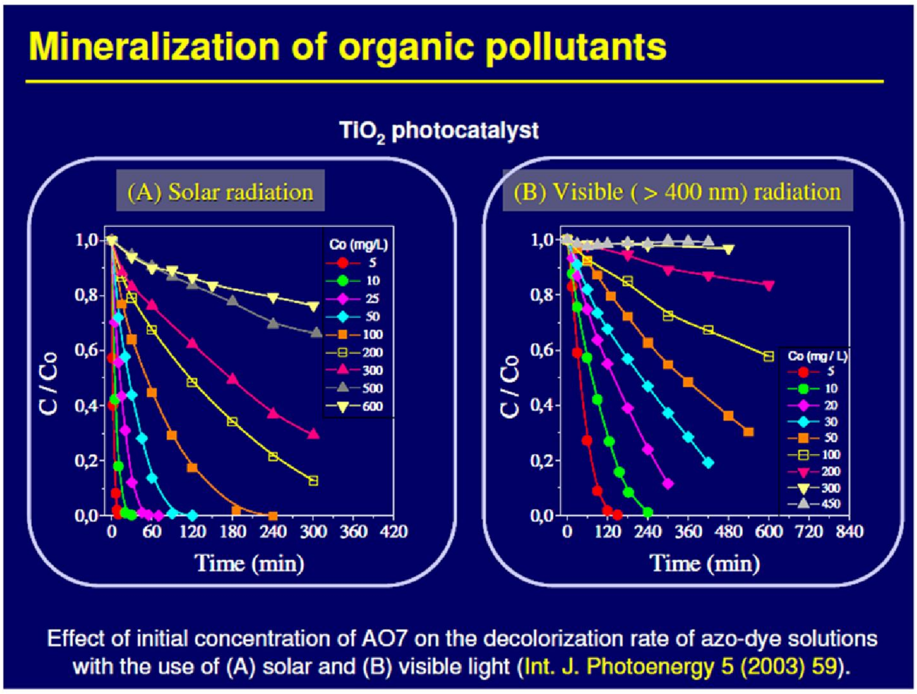

Mineralization of organic pollutants

TiO_2 photocatalyst

Effect of initial concentration of AO7 on the decolorization rate of azo-dye solutions with the use of (A) solar and (B) visible light (Int. J. Photoenergy 5 (2003) 59).

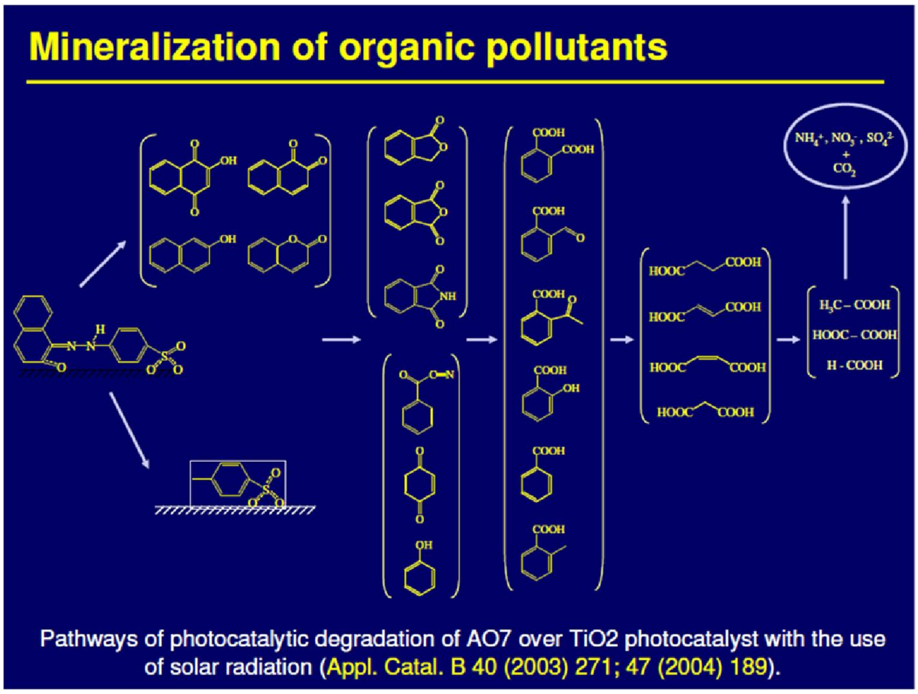

Mineralization of organic pollutants

Pathways of photocatalytic degradation of AO7 over TiO2 photocatalyst with the use of solar radiation (Appl. Catal. B 40 (2003) 271; 47 (2004) 189).

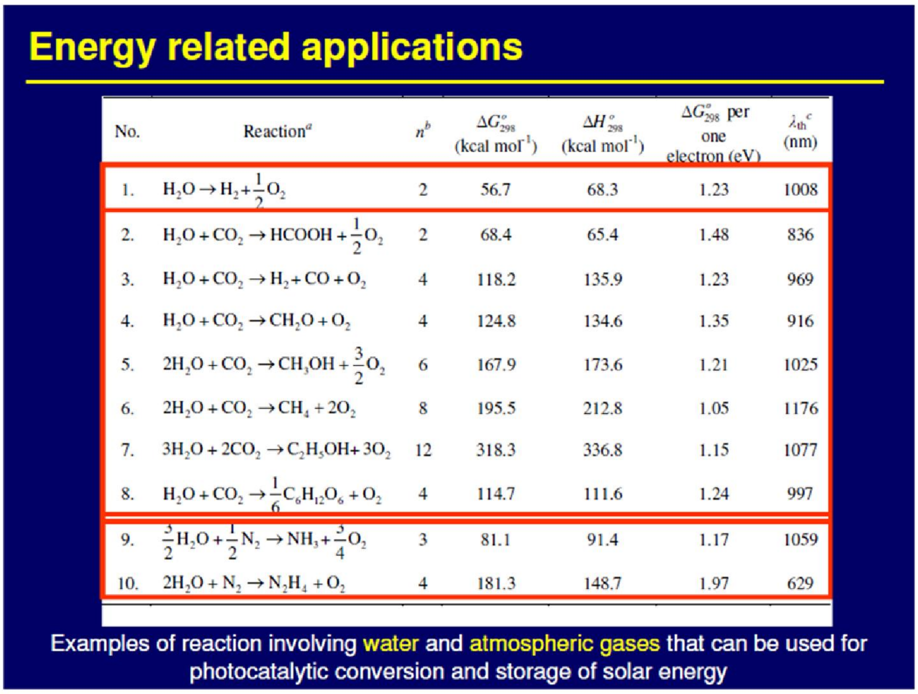

Energy related applications

No.	Reaction[a]	n[b]	ΔG^{o}_{298} (kcal mol^{-1})	ΔH^{o}_{298} (kcal mol^{-1})	ΔG^{o}_{298} per one electron (eV)	λ_{th}[c] (nm)
1.	$H_2O \rightarrow H_2 + \frac{1}{2}O_2$	2	56.7	68.3	1.23	1008
2.	$H_2O + CO_2 \rightarrow HCOOH + \frac{1}{2}O_2$	2	68.4	65.4	1.48	836
3.	$H_2O + CO_2 \rightarrow H_2 + CO + O_2$	4	118.2	135.9	1.23	969
4.	$H_2O + CO_2 \rightarrow CH_2O + O_2$	4	124.8	134.6	1.35	916
5.	$2H_2O + CO_2 \rightarrow CH_3OH + \frac{3}{2}O_2$	6	167.9	173.6	1.21	1025
6.	$2H_2O + CO_2 \rightarrow CH_4 + 2O_2$	8	195.5	212.8	1.05	1176
7.	$3H_2O + 2CO_2 \rightarrow C_2H_5OH + 3O_2$	12	318.3	336.8	1.15	1077
8.	$H_2O + CO_2 \rightarrow \frac{1}{6}C_6H_{12}O_6 + O_2$	4	114.7	111.6	1.24	997
9.	$\frac{3}{2}H_2O + \frac{1}{2}N_2 \rightarrow NH_3 + \frac{3}{4}O_2$	3	81.1	91.4	1.17	1059
10.	$2H_2O + N_2 \rightarrow N_2H_4 + O_2$	4	181.3	148.7	1.97	629

Examples of reaction involving water and atmospheric gases that can be used for photocatalytic conversion and storage of solar energy

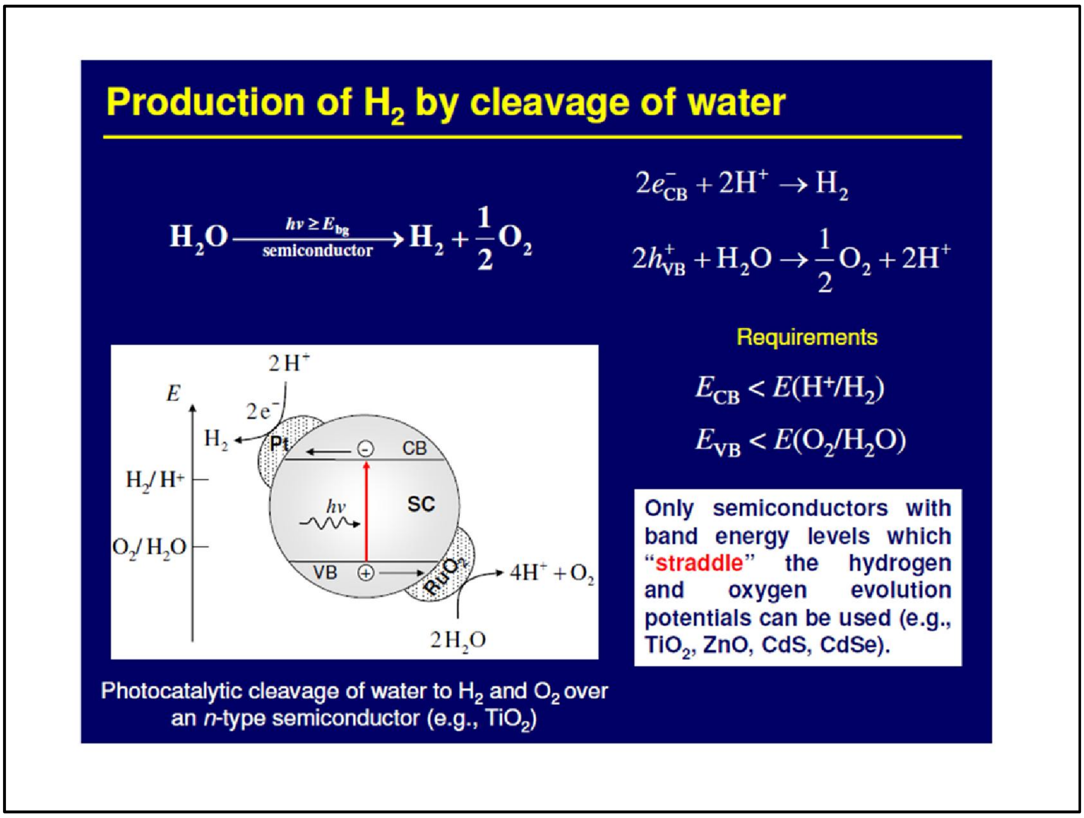

Production of H_2 by cleavage of water

$$H_2O \xrightarrow[\text{semiconductor}]{h\nu \geq E_{bg}} H_2 + \frac{1}{2}O_2$$

$$2e^-_{CB} + 2H^+ \rightarrow H_2$$

$$2h^+_{VB} + H_2O \rightarrow \frac{1}{2}O_2 + 2H^+$$

Photocatalytic cleavage of water to H_2 and O_2 over an *n*-type semiconductor (e.g., TiO_2)

Requirements

$$E_{CB} < E(H^+/H_2)$$

$$E_{VB} < E(O_2/H_2O)$$

Only semiconductors with band energy levels which "straddle" the hydrogen and oxygen evolution potentials can be used (e.g., TiO_2, ZnO, CdS, CdSe).

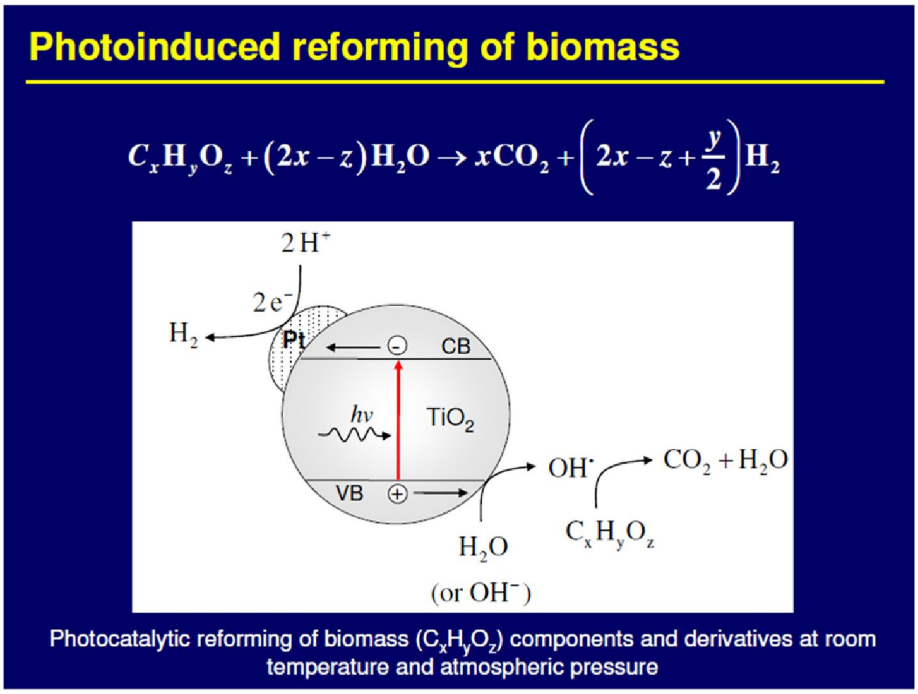

Photoinduced reforming of biomass

$$C_xH_yO_z + (2x - z)H_2O \rightarrow xCO_2 + \left(2x - z + \frac{y}{2}\right)H_2$$

Photocatalytic reforming of biomass ($C_xH_yO_z$) components and derivatives at room temperature and atmospheric pressure